Postseismic deformation in Pakistan after the 8 October 2005 earthquake: Evidence of afterslip along a flat north of the Balakot-Bagh thrust

F. Jouanne,[1] A. Awan,[2] A. Madji,[2] A. Pêcher,[3] M. Latif,[2] A. Kausar,[2] J. L. Mugnier,[1] I. Khan,[4] and N. A. Khan[2]

Received 1 August 2010; revised 15 December 2010; accepted 14 April 2011; published 7 July 2011.

[1] The 8 October 2005 Kashmir earthquake ruptured an out-of-sequence Himalayan thrust known as the Balakot-Bagh thrust. The earthquake's hypocenter was located at a depth of 15 km on the ramp close to a possible ramp/flat transition. In the weeks following the earthquake a GPS network was installed to measure postseismic displacement. The initial measurements in November 2005 were followed by other campaigns in January and August 2006, in March and December 2007, and in August 2008 and 2009. Two hypotheses were tested: post-seismic displacements controlled by viscous relaxation of the lower crust or by afterslip along a flat north of the ramp affected by the main shock. A single Newtonian viscosity for the different periods cannot be determined by numerical simulations of viscous relaxation, which may indicate that the viscosity of the lower crust is non-Newtonian or that viscous relaxation does not control postseismic displacements. Numerical simulations using dislocations in a uniform elastic half-space indicate afterslip north of the ramp of the earthquake along a flat connected to the ramp. Slip along the northwestern portion of the flat accrued to about 285 mm between November 2005 and August 2006, while slip along the southeastern portion accrued to 130 mm over the same time period. Residual misfit of the observed and predicted displacements clearly indicated that afterslip is a better explanation for the observations than the hypothesis of viscous relaxation. The time evolution of the afterslip was found to be consistent with that predicted from rate-strengthening frictional sliding.

Citation: Jouanne, F., A. Awan, A. Madji, A. Pêcher, M. Latif, A. Kausar, J. L. Mugnier, I. Khan, and N. A. Khan (2011), Postseismic deformation in Pakistan after the 8 October 2005 earthquake: Evidence of afterslip along a flat north of the Balakot-Bagh thrust, *J. Geophys. Res.*, *116*, B07401, doi:10.1029/2010JB007903.

1. Introduction

[2] On 8 October 2005 the western Himalaya were affected by an *Mw* 7.6 earthquake. This event occurred along the Balakot-Bagh thrust, a 30°-dipping ramp [*Avouac et al.*, 2006] located above the gently dipping main Himalayan thrust (MHT), at more than 150 km to the northeast of the main frontal thrust (MFT). This seismic event therefore occurred in an out-of-sequence structural location with respect to the Himalayan thrust system, whereas other large Himalayan earthquakes are located along the main Himalayan thrust, with ruptures reaching the surface in certain cases [*Mugnier et al.*, 2004; *Lavé et al.*, 2005; *Kumar et al.*, 2006]. The Balakot-Bagh thrust has been ruptured by 32 m vertical throw since the last glacial maximum [*Kaneda et al.*, 2008], which corresponds to a 1.4–4.1 mm/yr mean horizontal displacement and to 9–10 ruptures similar to the Balakot event since 10–30 ka. This thrust absorbs only a fraction of the 16–18 mm/yr shortening expected across the western Himalaya [*Jade et al.*, 2004].

[3] The 8 October 2005 event is the first earthquake in the Himalaya with documented surface rupture. It is also the first large Himalayan earthquake since the advent of GPS geodesy. Therefore it is a unique opportunity to study great earthquakes in an intracontinental collision belt. After the earthquake, a GPS network was installed to monitor the postseismic displacements. The monitoring strategy was defined in such a way as to identify the spatial and temporal evolution of the postseismic displacements and to take into account difficulties due to logistical and political constraints. The geodetic data are compared to seismological data and to mechanical models in order to assess the mechanisms con-

[1] ISterre, UMR 5275, Université de Savoie, CNRS, Le Bourget du Lac, France.
[2] Geological Survey of Pakistan, Islamabad, Pakistan.
[3] ISterre, UMR 5275, Université Joseph Fourier, CNRS, Grenoble, France.
[4] Geological Survey of Pakistan, Quetta, Pakistan.

0148-0227/11/2010JB007903

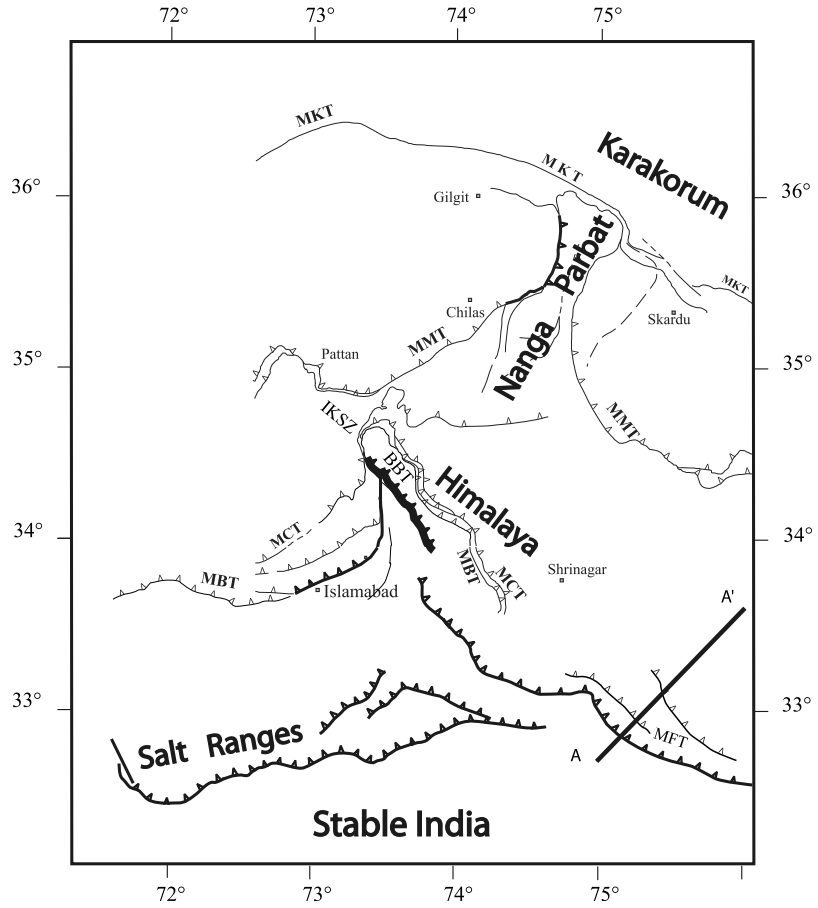

Figure 1. Structural scheme of active faults in the western Himalaya. Active structures are shown as thick black lines. The Balakot-Bagh thrust (BBT) ruptured by the 8 October 2005 earthquake is indicated with a thicker line. MFT, main frontal thrust; MBT, main boundary thrust; MCT, main central thrust; MMT, main mantle thrust; IKSZ, Indus-Kohistan seismic zone.

trolling the seismotectonic behavior and rheology of major thrusts in intracontinental collision belt.

2. Geological Setting

[4] The Himalayan belt is a large accretionary wedge built from the northern Indian continental crust after the Indian-Tibetan collision during the Middle Eocene. After the collision, the average India-Asia convergence rate is estimated to be 4 cm/yr [*Bettinelli et al.*, 2006]. On the Indian side, it is accommodated by the stacking of several thrust sheets of XX km thick scales, separated by thrusts (MCT, MBT and MFT). In the central Himalaya, three main thrusts accommodate most of the displacement; namely from north to south: (1) the MCT, which brings the Higher Himalayan Crystalline Massifs onto the Lesser Himalaya; (2) the MBT, along which the Lesser Himalaya overrides the Siwalik Miocene detrital series; and (3) the MFT between the Siwaliks and the Plio-Quaternary deposits of the Ganges plain.

3. Balakot-Bagh Thrust

[5] The Balakot-Bagh thrust may be defined as a NW-SE thrust system ranging from the Indus Valley (Besham area) to the Jhelum Valley in Kashmir (Figure 1). Its geological signature is not major, but it accounts for the 8 October 2005 Kashmir earthquake (Figure 2). It seems that this thrust corresponds to a ramp dipping 30°NE, connected to a flat, which could be an equivalent of the central Himalayan MHT, above which spreads the piggyback basin of Kashmir (Figure 3). The Balakot-Bagh thrust could be prolonged at depth toward the northeast in the floor thrust of a blind wedge [*Bendick et al.*, 2007] and probably accounts for the 1974 M_S 6.2 Pattan earthquake that took place along the ramp [*Pennington*, 1989] rather than on a flat thrust. Toward the southeast, the prolongation of the Balakot-Bagh thrust could be the Kotli-Riasi thrust [*Jayangondaperumal and Thakur*, 2008] (Figure 1).

[6] The recent tectonics of the Balakot-Bagh thrust has been investigated using topographic profiles of the cumulative fault scarp that affects the top of a fill terrace assumed to be associated with the last glacial maximum [*Kaneda et al.*, 2008]. The cumulative scarp indicates the occurrence of 9–10 similar earthquakes since the creation of this surface. Assuming an age between 10 and 30 ka, this observation suggests a recurrence of earthquakes similar to the 8 October 2005 earthquake of 1000–3300 years and a 1.4–4.1 mm/yr mean horizontal displacement along this fault [*Kaneda et al.*,

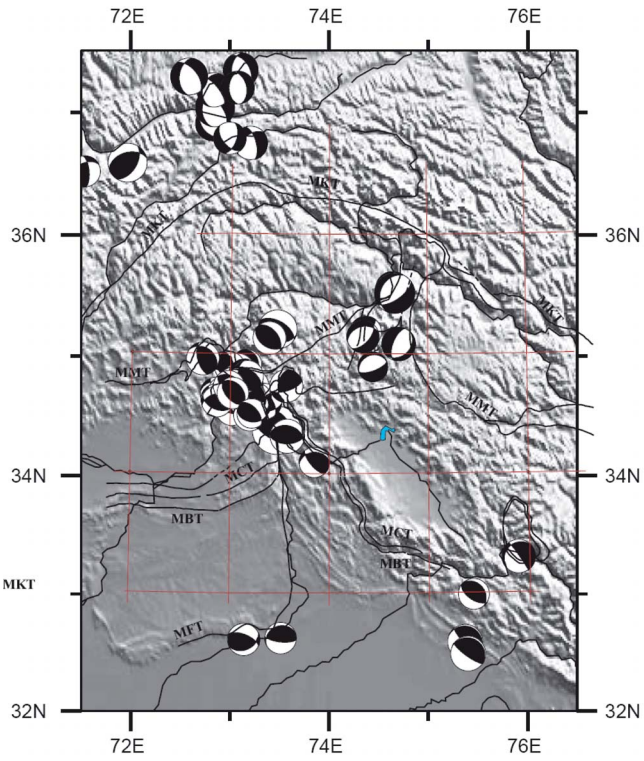

Figure 2. Focal mechanism of earthquakes prior to the 8 October 2005 earthquake and of main aftershocks following this last event.

2008]. This estimated mean horizontal displacement is much smaller than the Himalayan shortening, which is estimated to be 18.8 ± 3 mm/yr between Ladakh and the Indian subcontinent [*Jade et al.*, 2004]. This observation suggests that the Balakot-Bagh thrust is not the main thrust of the western Himalaya.

[7] In the Hazara syntaxis, the MCT and MBT are clearly inactive and are like passive markers displaced by the activity of the Balakot-Bagh thrust. The Indus-Kohistan seismic zone, the Patan 1974 (*Mw* = 6.2) earthquake and the aftershock distribution following the 8 October 2005 earthquake (Figure 2) indicate that the area northwest of the Balakot-Bagh thrust is characterized by several active thrusts with the same direction as the Balakot-Bagh thrust. These active thrusts are not associated with clear morphological signatures. This can be interpreted as indicating an immature structure linked to the northwestward lateral propagation of the Balakot-Bagh thrust. This suggests that the current termination of the cylindrical Himalayan belt is west of the Indus, in the area of the structures described as a syntaxis by *DiPietro et al.* [1999].

4. The 8 October 2005 Earthquake

[8] Kashmir and northern Pakistan were affected by a large-magnitude earthquake (*Mw* 7.6) on 8 October 2005 (Figure 1). This earthquake, the most devastating to have occurred in the Himalaya, claimed at least 80,000 lives. The rupture area has been studied by field investigations [*Kaneda et al.*, 2008], by optical [*Avouac et al.*, 2006] or SAR [*Pathier et al.*, 2006] quantification of ground deformation and by inversion of teleseismic body waves (see http://www.emsc-csem.org/; https://geoazur.oca.eu/spip.php?article112; http://www.geol.tsukuba.ac.jp/~yagi-y/EQ/2005Pakistan/index.html; http://earthquake.usgs.gov/earthquakes/eqinthenews/2005/usdyae/finitefault/) [*Avouac et al.*, 2006]. The slip pattern of this earthquake appears to be a relatively simple, coseismic slip affecting a relatively steep crustal ramp (30°) between the surface and 15 km depth. The coseismic slip [*Avouac et al.*, 2006; *Pathier et al.*, 2006] reached maximum just north of Muzafarabad with displacements up to 9.6 m at 4 km depth located beneath the Muzafarabad-Balakot ramp [*Pathier et al.*, 2006], in the core of the Hazara syntaxis outlined by the hairpin bend of the main boundary thrust and ending abruptly north of Balakot (Figure 1), where this fault seems to disappear. Nonetheless, the Indus-Kohistan Seismic Zone could relay the Muzafarabad fault northwest of Balakot [*Armbruster et al.*, 1978; *Seeber and Armbruster*, 1979; *Seeber et al.*, 1981]. There is no clear consensus on the slip distribution. *Avouac et al.* [2006] assume the existence of a single asperity above the hypocenter with a maximum of 9 m displacement north of Muzafarabad whereas other studies propose two major asperities [*Parsons et al.*, 2006] or multiple asperities [*Fujiwara et al.*, 2006]. For example, *Pathier et al.* [2006] propose a slip distribution pattern for the Balakot-Muzafarabad ramp with slip affecting the entire ramp between the surface and 15 km depth, greater than 6 m between the surface and 12 km depth with a maximum reaching 9 m at 4 km depth, whereas the second segment south of Muzafarabad, the Muzafarabad-Tanda ramp,

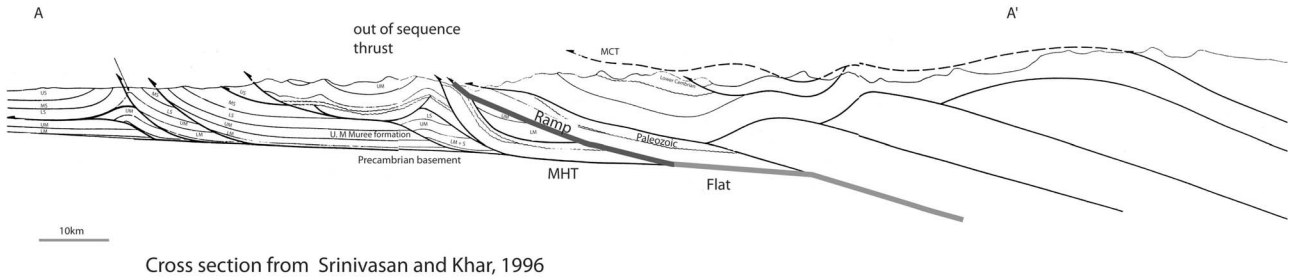

Figure 3. Cross section located east of the study area (location in Figure 1) illustrating the existence of an out-of-sequence thrust in the western Himalaya and the succession of ramps connecting to a single flat in the main Himalayan thrust.

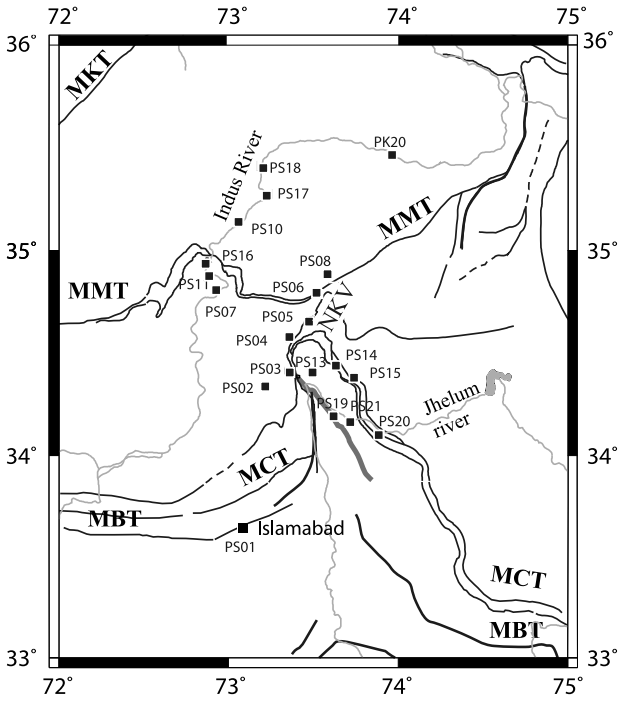

Figure 4. GPS network installed to measure postseismic displacements consecutive to the 8 October 2005 Kashmir earthquake.

is ruptured by less severe coseismic slip located between the surface and 10 km depth, with a peak of 7 m at 4 km depth.

5. Data Collection and Processing

[9] After the 8 October 2005 Kashmir earthquake, 18 benchmarks were installed and measured during the first week of November (see Table 1 and Figure 4), just after the road was reopened into the Narhan-Kaghan, Neelum and upper Jhelum valleys. In January 2006, large landslides cut the access to the Narhan-Kaghan and Neelum valleys, and new points were set up along the Indus Valley to document the occurrence of postseismic displacements in the Indus Kohistan seismic zone affected by a large number of aftershocks and in the upper Jhelum Valley to determine postseismic displacements along the southeastern part of the Balakot-Bagh thrust (Figure 4). Measurements were taken from the network again in August 2006, March 2007, December 2007, and August 2008 and 2009 at a few points in order to monitor the decrease in postseismic displacements (Table 1).

[10] Results were obtained using IGS final precise orbits [*Beutler et al.*, 1999], as recommended by *Boucher et al.* [2004], as well as IGS Earth rotation parameters and data from nearby permanent GPS stations. The absolute antenna phase centre offsets models were used.

[11] Data were analyzed using the following strategy: (1) initial ionosphere-free analysis with computation of residuals, (2) residuals analysis, (3) resolution of wide-lane ambiguities using the Melbourne-Wübbena linear combination [*Melbourne*, 1985; *Wübbena*, 1985] with DCB files when available, (4) computation of the ionosphere-free solution introducing the resolved Melbourne-Wübbena linear combination ambiguities, and (5) computation of the normal equations. Troposphere-induced propagation delays were estimated from observations made every 2 hours. Each daily solution was transformed in the ITRF2005 [*Altamimi et al.*, 2007] reference frame with a seven-parameter Helmert solution. Coordinates and velocities were then estimated using the Bernese 5.0 software in the ITRF2005 reference frame.

[12] Finally, velocities were expressed relative to the point installed in Islamabad (point PS01, Geological Survey of Pakistan Office in Islamabad), enabling displacements to be expressed relative to the northern Potwar Basin, south of the Balakot-Bagh thrust but north of the Himalayan front coinciding with the Salt Ranges frontal thrust (Table 2). The uncertainties estimated from analyzing the normal equations assume a white noise source of error. It has long been recognized that the main source of error in GPS time series is in fact a flicker noise [*Zhang et al.*, 1997]. *Williams et al.*

Table 1. Measurements From the GPS Network Dedicated to Postseismic Displacement Quantification

	Latitude	Longitude	November 2005	January 2006	August 2006	March 2007	December 2007	August 2008	August 2009
PS01	33.67	73.06	*	*	*	*	*	*	*
PS02	34.34	73.22	*	*	*				
PS03	34.42	73.36	*		*	*	*	*	*
PS04	34.35	73.36	*	*	*	*	*	*	*
PS05	34.66	73.48	*		*	*			*
PS06	34.79	73.52	*		*	*	*		
PS07	34.34	72.94	*	*	*	*			
PS08	34.87	73.61	*		*			*	
PS09	35.07	72.95		*		*			
PS10	35.14	73.06	*		*	*			
PS11	34.34	72.90	*	*	*	*			
PS13	34.33	73.48	*	*	*	*	*		*
PS14	34.44	73.63	*		*	*	*		
PS15	34.40	73.72	*			*			
PS16	34.35	72.88	*	*	*	*			
PS17	35.33	73.22		*	*				
PS18	35.35	73.20		*	*	*			
PS19	34.34	73.67		*	*	*	*		*
PS20	34.35	73.87		*	*				*
PS21	34.35	73.72		*	*	*	*		*
PK20	35.47	73.96			*	*			

Table 2. Displacement Rates Estimated for Point PS01 in the ITRF2005 Reference Frame and in the India Reference Frame

	ITRF2005		India Fixed			
	Evel	N vel	Evel	N vel	σe	σn
PS01	29.4	32.2	1.12	−2.14	0.5	0.5

[2004] show that flicker noise is 2–3 times higher than the corresponding white noise level. On the basis of this observation, we increased our formal error estimated, assuming white noise, by a factor of 3 (Table 2).

6. Results

[13] The numerous observations collected at point PS01 (see Figure 5 and Table 3) may be used to determine the displacement rate in the ITRF2005 reference frame and, in a second step, in the India fixed reference frame using the rotation pole proposed by *Altamimi et al.* [2007] (Table 2). The displacement rate of point PS01 is only 2.4 mm/yr southeastward (Table 2). There is therefore no clear difference between PS01 and the India fixed reference for the major postseismic displacements and it appears that the current displacement between PS01 and stable India, in both sides of the Potwar plateau and Salt Ranges thrust, is considerably less than the expected 6 ± 2 mm/yr [*McDougall and Khan*, 1990; *McDougall et al.*, 1993; *Grelaud et al.*, 2002; *Mugnier et al.*, 2008] deduced from neotectonics studies.

[14] The displacements measured for the period November 2005 to August 2006 (see Figure 6 and Table 3) enable postseismic displacements to be mapped with points in the Narhan-Kaghan and Neelum Valley. A most interesting result is the difference in orientation of the postseismic displacements between the northern segment and the southern segment of the Balakot-Bagh thrust, and the major displacements in the Narhan-Kaghan Valley at points located far from the emergence of the fault but also far from the connection between the ramp and the detachment level.

[15] During the second period between January 2006 and August 2006 (see Figure 7 and Table 3), displacements clearly decreased and postseismic displacements along the southern segment of the Balakot-Bagh thrust appear to have been very small. This lack of postseismic displacement along this segment is also underlined by the lack of recorded aftershocks southeast of the rupture area, whereas postseismic displacements are still significant along the northern segment of the Balakot-Bagh thrust.

[16] Displacements measured for the period August 2006 to March 2007 (Figure 8) illustrate the postseismic decrease at nearly all the points, with the exception of those located in the upper Narhan-Kaghan and Jhelum valleys that were unreachable because of the occurrence of numerous landslides. However, displacements measured between March and December 2007 and between August 2008 and August

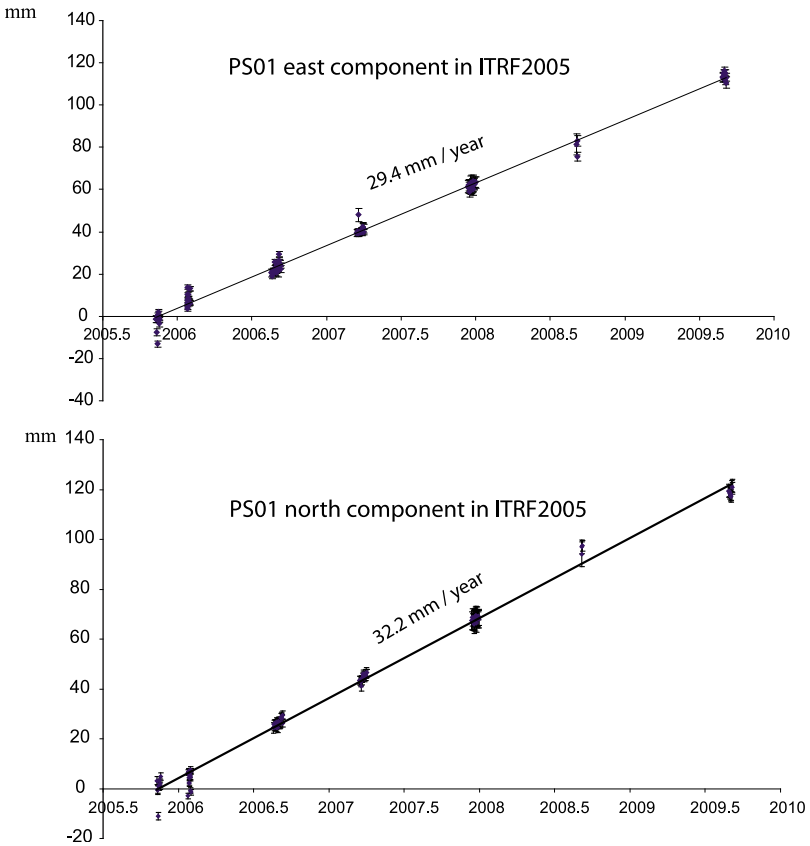

Figure 5. Time series of GPS point PS01 installed in Islamabad expressed in the ITRF2005 reference frame.

Table 3. Postseismic Displacements Estimated for Different Periods Expressed Relative to PS01

	Longitude	Latitude	East (mm)	North (mm)	Up (mm)	σe (mm)	σn (mm)	σu (mm)
				November 2005 to August 2006				
PS01	73.0642	33.6749	0.0	0.0	0.0	0.0	0.0	0.0
PS02	73.2196	34.3449	−7.7	−6.3	−2.1	3.2	2.4	11.1
PS03	73.3563	34.4221	−17.2	−15.6	−2.0	2.4	1.6	9.5
PS04	73.3620	34.5785	−56.9	10.5	54.6	4.0	3.2	14.3
PS05	73.4761	34.6602	−50.0	−29.8	−25.4	5.5	4.8	22.2
PS06	73.5185	34.7887	−16.8	−37.5	−8.6	6.3	5.5	35.6
PS07	72.9360	34.8023	2.7	−4.8	22.8	2.4	2.4	10.3
PS08	73.6114	34.862	−23.5	−41.5	12.8	5.5	4.0	16.6
PS10	73.0617	35.1387	−2.1	−9.3	1.6	4.8	4.0	20.6
PS11	72.9002	34.8768	−3.3	−3.2	2.1	4.8	3.2	15.0
PS13	73.4850	34.4171	−28.5	−11.4	0.2	4.8	4.0	23.0
PS14	73.6333	34.4394	−25.4	−37.9	41.3	3.2	2.4	15.0
PS16	72.8763	34.9320	4.7	−18.1	19.7	4.8	4.0	17.4
				November 2005 to March 2007				
PS01	73.0642	33.6749	0.0	0.0	0.0	0.0	0.0	0.0
PS02	73.2196	34.3449	−22.2	−13.6	5.4	1.4	2.7	8.1
PS03	73.3563	34.4221	−19.4	−17.8	−18.7	1.4	1.4	8.1
PS04	73.3620	34.5785	−64.6	4.9	48.6	2.7	2.7	10.8
PS05	73.4761	34.6602	−63.1	−41.1	−30.9	5.4	5.4	23.1
PS06	73.5185	34.7887	−27.9	−50.9	17.0	6.8	6.8	33.9
PS07	72.9360	34.8023	2.0	−3.9	−4.1	2.7	2.7	9.5
PS09	72.9543	35.0676	4.7	−10.8	643.1	4.1	2.7	17.6
PS10	73.0617	35.1387	−7.1	−16.0	−40.1	4.1	5.4	20.3
PS11	72.9002	34.8768	−1.2	−8.3	4.2	2.7	4.1	13.6
PS13	73.4850	34.4171	−34.9	−14.5	45.7	4.1	4.1	23.1
PS14	73.6333	34.4394	−33.4	−57.0	48.7	2.7	4.1	14.9
PS15	73.7182	34.4004	−11.3	−56.6	20.5	5.4	4.1	23.1
PS16	72.8763	34.9320	4.3	−15.2	−1.1	4.1	4.1	16.3
				January–August 2006				
PS01	73.0642	33.6749	0.0	0.0	0.0	0.0	0.0	0.0
PS02	73.2196	34.3449	−4.5	−1.9	−10.3	2.4	2.9	10.6
PS04	73.3620	34.5785	−35.7	8.7	18.8	3.5	4.1	15.9
PS07	72.9360	34.8023	1.1	−11.9	20.3	2.9	3.5	13.5
PS11	72.9002	34.8768	−4.7	−10.0	0.8	2.9	4.1	14.7
PS13	73.4850	34.4171	−23.5	−13.4	−41.7	4.7	4.7	22.4
PS16	72.8763	34.9320	−5.2	−19.8	21.0	3.5	3.5	15.9
PS17	73.2229	35.2676	−6.4	−8.7	−62.4	3.5	4.1	20.6
PS18	73.2013	35.3993	−3.9	−15.8	13.9	4.7	4.7	23.0
PS19	73.6653	34.1902	−3.8	−10.9	−16.1	2.4	2.9	11.8
PS20	73.8657	34.1296	−2.9	−12.1	2.1	2.9	2.9	13.5
PS21	73.7172	34.1788	−3.2	−14.9	5.3	2.4	3.5	13.0
				January 2006 to March 2007				
PS01	73.0642	33.6749	0.0	0.0	0.0	0.0	0.0	0.0
PS04	73.362	34.5785	−43.0	3.0	13.7	2.3	3.5	12.7
PS07	72.936	34.8023	0.6	−11.0	−7.8	3.5	3.5	12.7
PS09	72.9543	35.0676	−2.0	−6.8	610.3	3.5	3.5	16.1
PS11	72.9002	34.8768	−2.7	−15.0	1.3	3.5	3.5	12.7
PS13	73.485	34.4171	−29.9	−16.6	6.2	4.6	4.6	21.9
PS16	72.8763	34.932	−5.4	−17.0	−1.6	3.5	3.5	13.8
PS18	73.2013	35.3993	−7.3	−17.1	−11.1	3.5	3.5	17.3
PS19	73.6653	34.1902	−5.7	−18.5	0.8	2.3	2.3	12.7
PS21	73.7172	34.1788	−9.6	−16.5	3.3	3.5	3.5	11.5
				August 2006 to March 2007				
PS01	73.0642	33.6749	0.0	0.0	0.0	0.0	0.0	0.0
PK20	73.9644	35.4713	−2.5	−11.6	−20.3	3.4	4.0	16.4
PS03	73.3563	34.4221	−2.0	−2.1	−16.8	2.3	2.3	9.0
PS04	73.3620	34.5785	−7.1	−5.8	−6.7	3.4	4.0	15.8
PS05	73.4761	34.6602	−12.6	−11.1	−5.4	2.8	4.0	15.8
PS06	73.5185	34.7887	−11.0	−13.1	26.6	4.0	3.4	20.3
PS07	72.9360	34.8023	−0.6	0.9	−26.2	2.3	2.8	11.3
PS10	73.0617	35.1387	−4.9	−6.7	−40.8	2.8	3.4	15.2
PS11	72.9002	34.8768	2.0	−5.1	2.1	2.3	2.8	10.7
PS13	73.4850	34.4171	−6.0	−2.9	46.3	3.4	3.4	18.1
PS14	73.6333	34.4394	−7.7	−18.9	6.8	2.8	3.4	15.2
PS16	72.8763	34.9320	−0.3	2.6	−20.3	2.8	2.8	12.4
PS18	73.2013	35.3993	−3.3	−1.5	−20.8	4.0	4.0	19.8
PS19	73.6653	34.1902	−1.7	−7.6	13.0	2.8	3.4	14.1
PS21	73.7172	34.1788	−6.5	−1.2	−6.7	2.8	3.4	13.0

Table 3. (continued)

	Longitude	Latitude	East (mm)	North (mm)	Up (mm)	σe (mm)	σn (mm)	σu (mm)
				March–December 2007				
PS01	73.0642	33.6749	0.0	0.0	0.0	0.0	0.0	0.0
PS03	73.3563	34.4221	−3.0	−3.3	31.4	5.3	3.8	22.6
PS04	73.3620	34.5785	−13.9	2.0	42.0	3.0	2.3	12.8
PS06	73.5185	34.7887	−6.9	−14.2	28.0	3.8	3.0	19.6
PS13	73.4850	34.4171	−12.9	−13.0	46.6	3.8	3.0	18.1
PS14	73.6333	34.4394	−8.7	−19.4	19.7	3.0	2.3	14.3
PS19	73.6653	34.1902	−6.3	−3.5	19.1	4.5	3.8	18.8
PS21	73.7172	34.1788	−6.3	−6.7	17.6	3.0	2.3	12.8
				March 2007 to August 2009				
PS01	73.0642	33.6749	0.0	0.0	0.0	0.0	0.0	0.0
PS03	73.3563	34.4221	−8.7	−3.4	17.7	2.4	2.4	7.3
PS05	73.4761	34.6602	−22.1	−18.2	60.5	2.4	2.4	14.6
PS13	73.4850	34.4171	−21.6	−11.4	48.4	2.4	2.4	14.6
PS19	73.6653	34.1902	−10.9	−4.9	23.6	2.4	2.4	14.6
PS21	73.7172	34.1788	−13.4	−9.0	6.3	2.4	2.4	9.7

2009 (see Figure 9 and Table 3) illustrate the slow decrease in postseismic motions.

7. Discussion

7.1. Modeling of Postseismic Displacements: Viscous Relaxation Hypothesis

[17] Here we test the hypothesis that the postseismic displacements are related to viscous relaxation of the middle and lower crust assumed to be located between 15 and 60 km depth. To test this hypothesis, we used the Visco1D software [*Banerjee et al.*, 2007; *Pollitz*, 1997, 2003]. We considered a thrust located between the surface and 15 km depth in the elastic upper crust. We supposed that this thrust had been affected by a uniform coseismic displacement of 4.2 m (mean displacement proposed by *Pathier et al.* [2006]). The lower crust between 15 and 60 km depth was supposed to have a uniform Newtonian viscosity whereas the mantle viscosity was fixed at 10^{19} Pa s. We determined the best fitting viscosity for the lower crust (between 5×10^{17} and 10^{21} Pa s) using displacements estimated for the time spans November 2005 to August 2006, August 2006 to March 2007, and March–August 2007 (Figure 10). The best values obtained for the lower-crust viscosity was 3×10^{18} Pa s for the first time span (November 2005 to August 2006), 15×10^{18} Pa s for the second (August 2006 to March 2007) and 30×10^{18} Pa s for the third (March 2007 to August 2009). In a second step, we have tested the influence of the mantle viscosity on the choice of the best value for the lower-crust viscosity. We have tested mantle viscosity of 10^{18} Pa s, 10^{19} Pa s, 10^{20} Pa s and 10^{21} Pa s for the three time spans. For the three time spans, the best misfit is obtained for a 10^{19}–10^{20} Pa s mantle viscosity, whereas viscosities of 10^{18} Pa s and 10^{21} Pa s are associated with larger misfits. The large and significant differences between the viscosity adjusted for the first time span and the other periods underline the fact that the relaxation of the lower crust, assumed to be a Newtonian body, cannot alone explain the postseismic displacements or that the viscosity of the lower crust is non-Newtonian. As the optimal lower-crust viscosity increases with postseismic time, a power law viscosity can be an explanation for this non-Newtonian behavior. Such behavior, where the strain rate is proportional to a power of stress has been proposed to explain apparent differences in viscosities proposed for different time spans following an earthquake [*Pollitz et al.*, 2001; *Chandrasekhar et al.*, 2009].

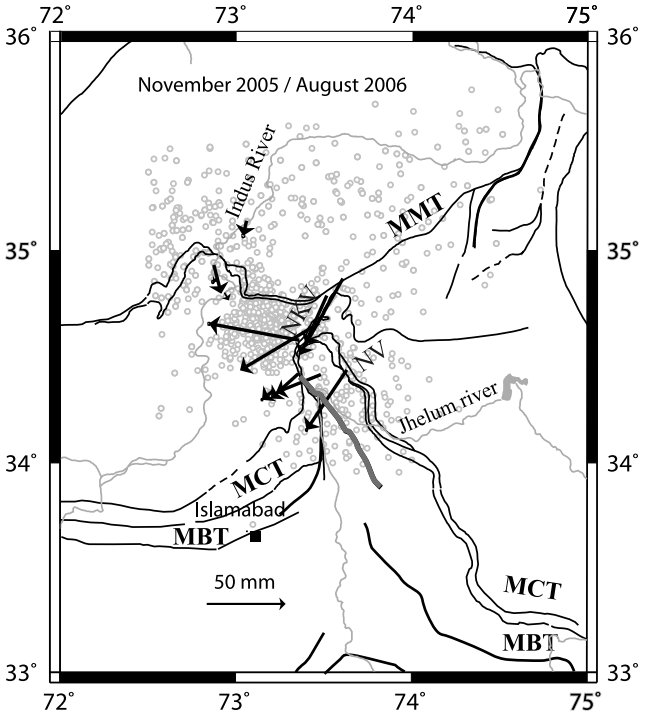

Figure 6. Postseismic displacements recorded between November 2005 and August 2006 expressed relative to Islamabad and seismicity recorded over the period considered. MBT, Main boundary thrust; MCT, main central thrust; MMT, main mantle thrust; NKV, Narhan-Kaghan Valley; NV, Neelum Valley. The Balakot-Bagh thrust is drawn with a thick line.

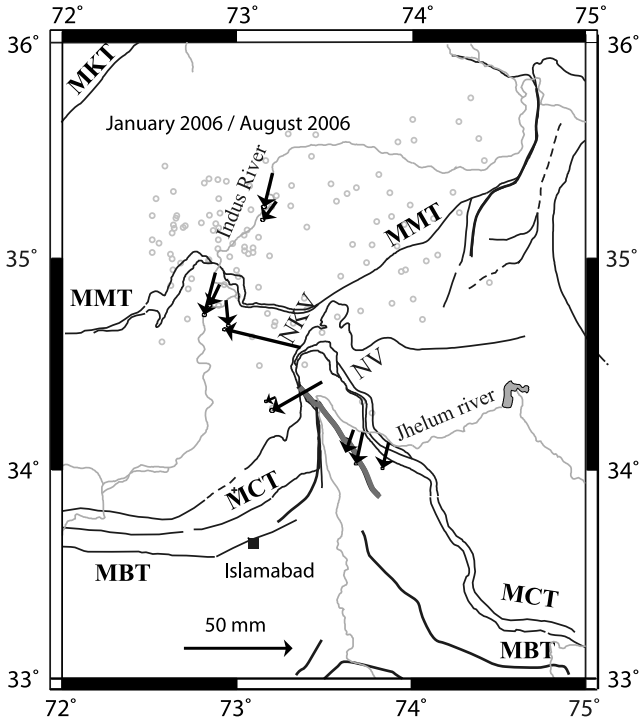

Figure 7. Postseismic displacements recorded between January 2006 and August 2006 expressed relative to Islamabad and seismicity recorded over the period considered. MBT, Main boundary thrust; MCT, main central thrust; MMT, main mantle thrust; NKV, Narhan-Kaghan Valley; NV, Neelum Valley. The Balakot-Bagh thrust is drawn with a thick line.

[18] Furthermore, the postseismic displacements occurring during the first year following the earthquake are not well modeled by relaxation of the middle and lower crust, as shown by the poor fitting between the observed and simulated displacements for the November 2005 to August 2006 time span (Figure 11). In particular, viscous relaxation is not able to simulate the observed obliquity between postseismic displacements and coseismic displacements (thrust without a strike-slip component), as observed at points located in the Narhan-Kaghan and Neelum valleys (Figure 11). In addition, viscous relaxation cannot predict the small and southward displacements observed at points located in the Indus River Valley. At these points the predicted and observed displacements are perpendicular (Figure 11).

7.2. Modeling of Postseismic Displacements: Afterslip Hypothesis

[19] It is assumed that the postseismic displacements are related to aseismic creep, which is modeled on the basis of the theory of a dislocation embedded in the elastic half-space. To do so we use the solution of *Okada* [1985] for a rectangular dislocation with uniform slip.

[20] These displacements can be linked to localized aseismic displacements along thrust planes considered as dislocations, and their upper tips correspond to a rheological or geometrical change in the thrust plane. It is assumed that the Balakot and Bagh ramps are connected at depth to a flat dipping 10° northeastward, as illustrated by a cross section [*Srinivasan and Khar*, 1996] located east of the study area (Figures 1 and 3) and as observed in the central Himalaya (connection of ramps to the main Himalayan thrust). The position of the flat-ramp transition is assumed to be at the foot of the ramp ruptured by the 8 October 2005 earthquake, at 15 km depth, which is consistent with the connection of the ramps along the MHT as illustrated on Figure 12.

[21] The strike of the dislocation is assumed to be parallel to the average structural direction of the Balakot-Bagh thrust. The segmentation of the fault used to define the dislocations was defined using structural data (Figures 3 and 12): a first dislocation represents the Balakot thrust (northwestern part of the Balakot-Bagh thrust ruptured by the 8 October 2005 earthquake), a second one represents the Bagh fault, the southern part of the active Balakot-Bagh thrust [*Avouac et al.*, 2006; *Kaneda et al.*, 2008], while two other dislocations represent flats assumed to follow the ramps modeled by the two first dislocations (Tables 4a and 4b). No major vertical postseismic displacements were measured during the postseismic phase and this lack for points northeast of the ramps reinforces the hypothesis that these points are located above thrust segments with moderate dips, referred to here as flats, that form the deeper parts of the active thrusts. The connection between the ramps and the flats is assumed to be at 15 km depth, at the foot of the ramp used to simulate coseismic displacements (see section 7.1). This is classically assumed to be the depth of the transition (Figure 12) between the brittle crust and the ductile crust.

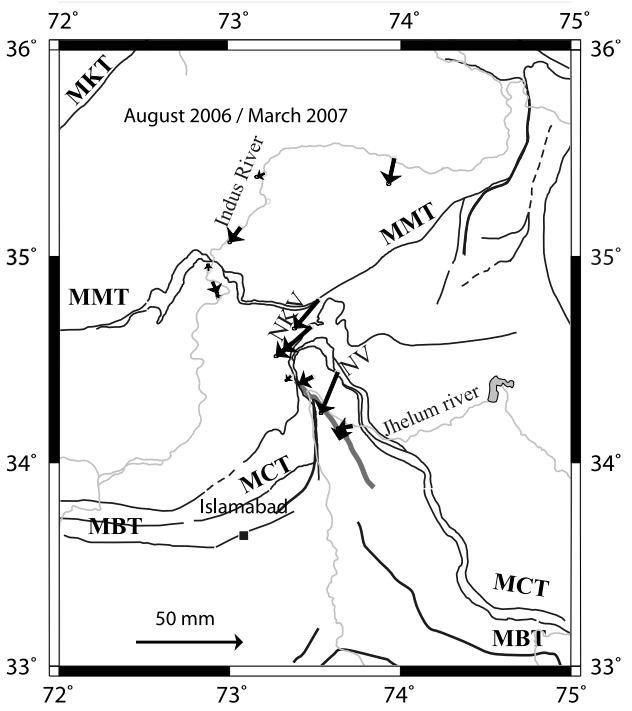

Figure 8. Postseismic displacements recorded between August 2006 and March 2007 expressed relative to Islamabad and seismicity recorded over the period considered. MBT, Main boundary thrust; MCT, main central thrust; MMT, main mantle thrust; NKV, Narhan-Kaghan Valley; NV, Neelum Valley. The Balakot-Bagh thrust is drawn with a thick line.

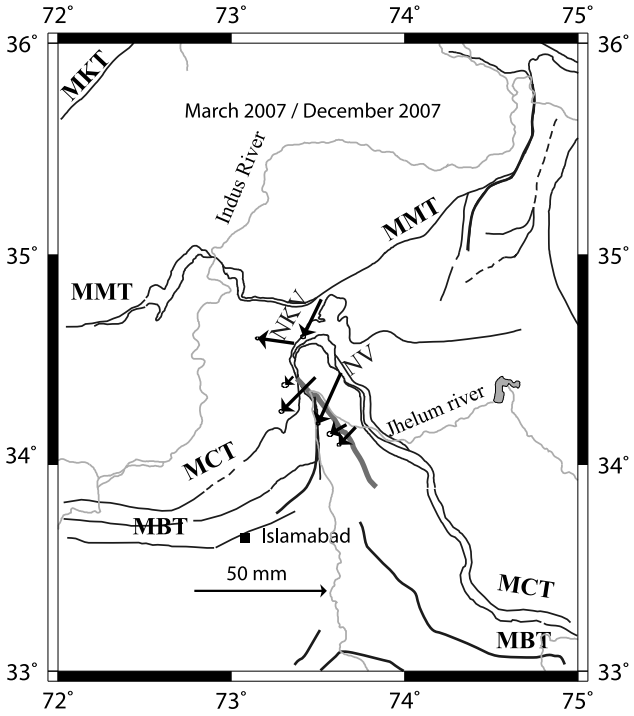

Figure 9. Postseismic displacements recorded between March and December 2007 expressed relative to Islamabad and seismicity recorded over the period considered. MBT, Main boundary thrust; MCT, main central thrust; MMT, main mantle thrust; NKV, Narhan-Kaghan Valley; NV, Neelum Valley. The Balakot-Bagh thrust is drawn with a thick line.

At 15 km depth, at a midcrustal level, the temperature is assumed to be higher than 250°C but not high enough to allow the development of ductile deformation, which occurs at temperatures higher than 400°C. At temperatures between 250 and 400°C, rate strengthening can be activated [*Blanpied et al.*, 1991, 1995; *Chester*, 1995; *Marone*, 1998; *Frye and Marone*, 2002; *Perfettini and Avouac*, 2004] allowing the existence of a brittle creeping part of the fault between the brittle part ($0 < T < 250$°C) and the ductile part ($T > 400$°C).

[22] To simulate displacements, we used a flat succeeding the Balakot thrust that is wider than the ramp, as suggested by the postseismic displacements recorded in the Narhan-Kaghan Valley north of Balakot. Thirty models were tested for each period. The best model is presented for which the sum of the weighted residuals (χ^2 test) between observed and simulated displacements is minimal (Tables 4a and 4b). Modeling of postseismic displacements for the November 2005 to August 2006 period (see Figure 13 and Table 5) indicates the occurrence of afterslip north of the ramps representing the Balakot and Bagh thrusts, along flats located at between 15 and 30 km depth (see section 7.3). The displacement reaches 308 mm along the northern flat, whereas along the southern flat it reaches 130 mm with a direction implying a thrust and dextral strike-slip components. The displacement of a point just near Balakot implies a moderate displacement along the Balakot thrust (88 mm), with a thrust component and a senestral strike-slip component, whereas the Bagh ramp is not affected by postseismic displacements. The comparison between coseismic slip (Figure 13a) and postseismic slip (Figure 13b) implies the existence of a significant obliquity between coseismic slip localized only along the ramp and postseismic slip localized mainly along the flat. Postseismic slip along the flats present an important dextral strike-slip component which is not the case for the coseismic slip that present a moderate dextral strike-slip component along the northwest part of the ramp and only a thrust component for the southeast part of the ramp.

[23] Modeling of the postseismic displacements for the August 2006 to March 2007 period (see Figure 14 and Table 5) indicates the occurrence of afterslip along the flats north of the ramps representing the Balakot and Bagh thrust fault. The displacement reaches 109 mm along the northern flat, whereas along the southern flat it reaches 60 mm with a direction of displacement implying a thrust and dextral strike-slip components. A good fit between the data and the model is obtained with no postseismic displacements along the Balakot and Bagh ramps during this period. Sensitivity tests were performed assuming a constant dip of the flat segment (Tables 4a and 4b) to study the extent, toward the north and toward the lower crust, of the zone with significant afterslip. This test was only performed for this time span, because the displacement of point PK20, north of the flat, is only available for this period. The best model indicates that the flat extends between 15 km (flat-ramp connection) and 30 km depth. It is therefore entirely in the lower crust and does not reach the mantle located at 60 km depth [*Rai et al.*, 2006].

[24] The measured postseismic displacements can thus be interpreted as being induced by afterslip along the flats located northeast of the Balakot-Bagh ramp. As was also shown by postseismic deformation consecutive to the Chi-Chi earthquake [*Yu et al.*, 2003; *Perfettini and Avouac*, 2004], afterslip affected mainly the part of the ramp-flat system that was unaffected during the main shock. This phenomenon was also observed in the case of the 1995 $Mw = 8.0$ Jalisco earthquake where afterslip occurred downdip of the coseismic rupture and migrated downward along the thrust plane [*Hutton et al.*, 2001]. In other cases, like the 2003 $Mw = 6.5$ Chengkung earthquake in eastern Taiwan [*Cheng et al.*, 2009; *Hsu et al.*, 2009] and the $Mw = 6.9$ Boumerdes earthquake in Algeria [*Mahsas et al.*, 2008], afterslip was also concentrated primarily in the fault plane area not ruptured by major coseismic displacement but upward to the coseismic slip patch.

[25] In the case of the 8 October 2005 earthquake, the afterslip affected the flat north of the ramp, with displacement being clearly oblique to the thrust, implying a major dextral strike-slip component, which did not occur during the earthquake (Figures 13 and 14). The afterslip direction along the flat appears to be parallel to the Himalayan shortening direction and not parallel to the main coseismic displacement.

[26] To analyze the time evolution of postseismic displacements, we analyzed the time evolution of afterslip and tested the model of *Perfettini and Avouac* [2004]. This model assumes that afterslip is governed by a rate-strengthening friction law. We also tested the hypothesis of *Perfettini and Avouac* [2004] that aftershocks are driven by afterslip by comparing the time evolution of both.

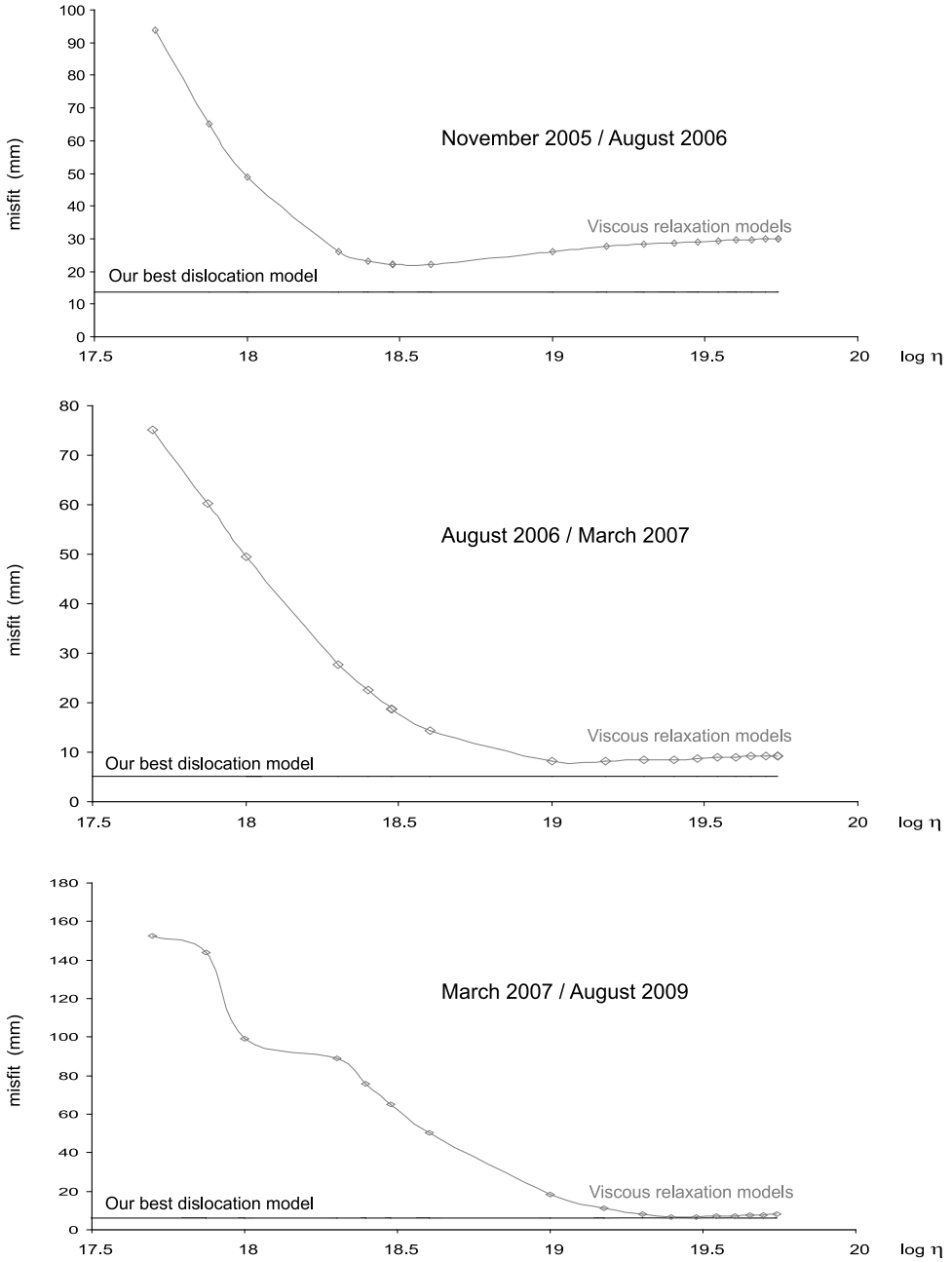

Figure 10. Residual misfits (in millimeters) between observed and simulated displacements for different lower-crust viscosity (χ^2 versus log η) and residual misfit obtained for our best dislocation model (see Table 5). Residual misfits were performed for the November 2005 to August 2006, August 2006 to March 2007, and March 2007 to August 2009 time spans using Visco1D-v3 software [*Banerjee et al.*, 2007; *Pollitz*, 1997, 2003].

[27] This model is defined by an analytical expression for the slip of the brittle creeping flat and has already been applied to the Chi-Chi earthquake [*Perfettini and Avouac*, 2004]. In particular, it successfully describes both the change in time of the aftershocks and the postseismic displacement time decay. This model predicts a logarithmic increase in slip that is dependent on the change in static Coulomb stress induced by the main shock. With the hypothesis that the seismicity rate may be considered to be proportional to the creep velocity along the flat, the model enables an aftershock decay rate to be proposed in accordance with Omori's law.

[28] The predicted change in postseismic displacement is expressed by the relation

$$U(t) = \alpha V_0 t + \beta V_0 t_r \log(1 + d(\exp(t/t_r) - 1) \qquad (1)$$

where V_0 is the interseismic displacement, α and β geometric factors and d = exp (ΔCFF/(aσ), where ΔCFF is the Coulomb stress change due to the earthquake and t_r the

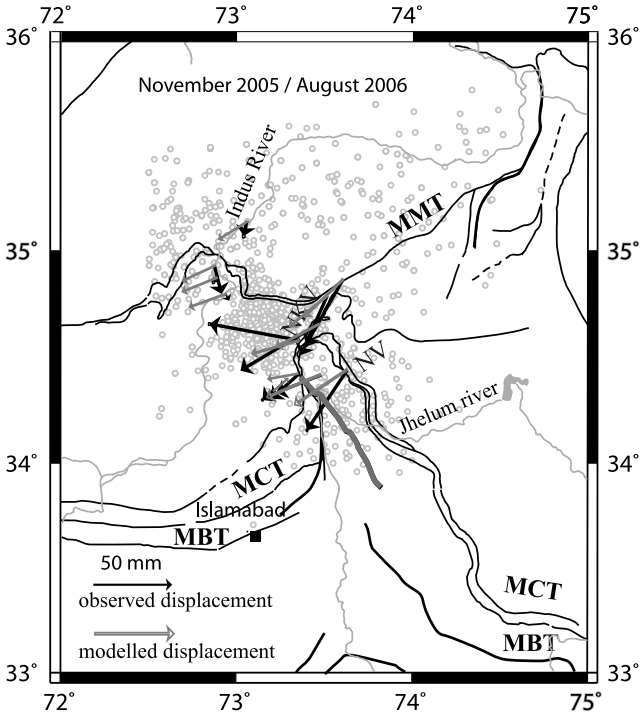

Figure 11. Modeling of displacements for the November 2005 to August 2006 period using Visco1D.v3 software to test the hypothesis of relaxation of the middle and lower crust as origin of observed postseismic displacements using a viscosity of 3×10^{18} Pa s (Figure 10).

characteristic time, $a = б\mu/б\log(V)$, μ being the coefficient of friction of the brittle creeping fault, V the displacement rate and σ the stress.

[29] If we assume, like *Perfettini and Avouac* [2004], a direct link between the postseismic displacement and the change in aftershocks with time, the number of aftershocks may be expressed as proposed by *Perfettini and Avouac* [2004] by:

$$N(t) = N_0 + R_0 t_r \log[1 + d(\exp(t/t_r) - 1)]$$

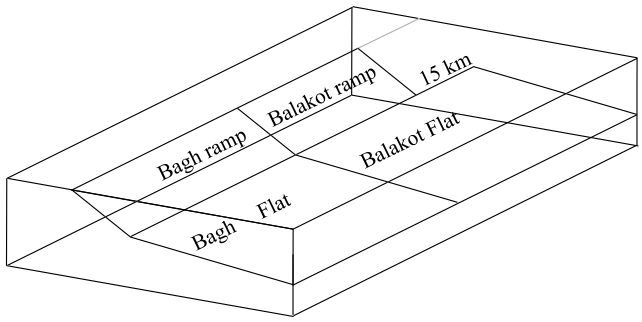

Figure 12. Set of dislocations used to model postseismic displacements. The segmentation of the thrust is based on the investigations of *Kaneda et al.* [2008] and *Avouac et al.* [2006]. The ramp is assumed to be connected to a flat dipping 10° northeastward.

Table 4a. Sensitivity Tests Performed to Determine the Extent of the Northeastern Flats[a]

Depth of Flats (km)	χ^2
15–25	5.18
15–30	5.15
15–35	5.16
15–40	5.23

[a]See Figure 12.

where N_0 is the number of aftershocks immediately following the main shock and R_0 the number of events per day. R_0, was determined using the ISC catalog (http://www.isc.ac.uk) by analyzing seismicity with mb > 3.5 for the years before the main shock ($R_0 = 0.08$ events per day).

[30] First, to determine the model parameters t_r and d, the microseismicity distribution through time following the 8 October 2005 earthquake is analyzed (Figure 15). The analysis suggests a characteristic time tr of 8.8 years and d = 3200.

[31] As shown in Figure 15, the evolution through time of the cumulative number of aftershock is well described by the period of observation of 600 days following the main shock. After 300 days, the predicted curve is nearly linear, we can then suppose that the 8.8 years characteristic time is valid although the observation period does not exceed 2 years, a quarter of the characteristics time.

[32] According to the model of *Perfettini and Avouac* [2004], the distribution of aftershocks and postseismic displacements must show the same time decay as the aftershocks induced by postseismic displacements.

[33] Second, the characteristic time tr was used to test whether the GPS time series changed in the same way. The geometrical parameters α and β linked with the GPS site location were determined for each time series and the fit between the observed and predicted time changes was tested using χ^2 value minimization (Figure 16). The observed and predicted displacements are consistent, which suggests a direct link between the time-dependent change in the postseismic displacements and the time-dependent aftershock distribution as proposed by *Perfettini and Avouac* [2004]. According to this model, and as observed postseismic displacements can be simulated by means of displacements along dislocations, it is highly likely that the time-dependent change in cumulated aftershocks is controlled by the occurrence of deep afterslip along the brittle creeping flat located north of the ramp ruptured by the 8 October 2005 quake. The occurrence of deep afterslip mainly along the flat located to the north the Balakot thrust may explain why the aftershocks are mainly located along the Indus Valley northeast of the Balakot thrust whereas only a few aftershocks were observed southwest of this thrust.

Table 4b. Geometrical Characteristics of the Dislocations Used to Model the Displacements

	Width (km)	Depth (km)	Dip	Strike
Northwestern ramp	20	5–15	30	142
Southeastern ramp	40	5–15	30	142
Northwestern flat	40	15–30	10	142
Southeastern flat	40	15–30	10	142

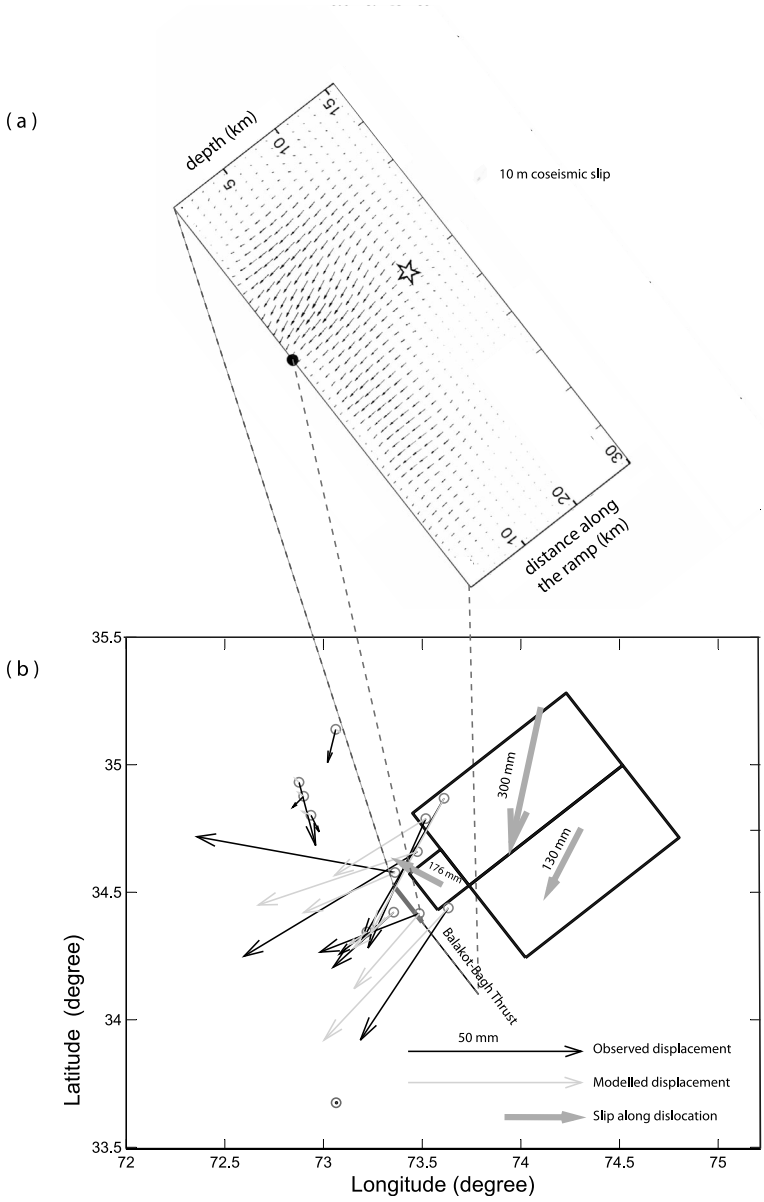

Figure 13. Coseismic slip [after *Pathier et al.*, 2006]. (a) Location of the NEIC epicenter (star). (b) Modeling of displacement using a set of four dislocations for the November 2005 to August 2006 period. The flat ramp transition is fixed at 15 km depth.

[34] As the observed and predicted displacements were consistent, we used the modeled time series to determine the total postseismic displacements for the 1500 days following the earthquake (Table 6). These displacements appear to be 3.7 times larger than the displacements observed for the November 2005 to August 2006 period (Table 6). To estimate the total moment released by afterslip along the dislocations, we then used slip estimated for the November 2005 to August 2006 period multiplied by 3.7.

[35] In this hypothesis of afterslip along flats, and if we consider an average elastic rigidity of 40 Gpa, a value that is compatible for the 0–15 km depth range, the moment

Table 5. Slip Along the Four Dislocations Used to Simulate Observed Postseismic Displacements for the Periods November 2005 to August 2006 and August 2006 to March 2007

	November 2005 to August 2006		August 2006 to March 2007	
	Right Lateral (mm)	Reverse (mm)	Right Lateral (mm)	Reverse (mm)
Northwestern ramp dip 30° (Balakot Ramp)	−79	39	0.00	0.00
Northwestern flat	198	237	57	85
Southeastern ramp dip 30° (Bagh Ramp)	0.00	0.00	0.00	0.00
Southeastern flat	55	118	28	40

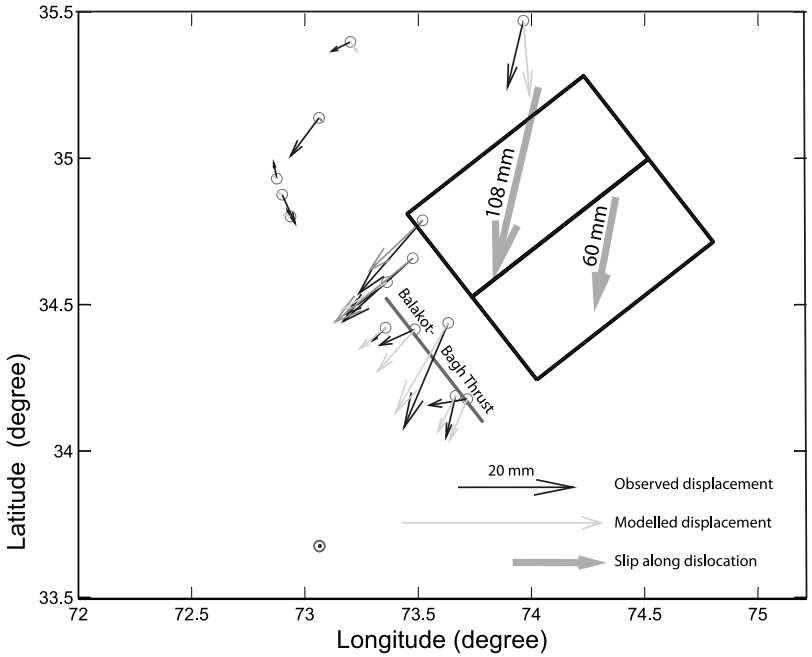

Figure 14. Modeling of displacement using a set of four dislocations for the August 2006 to March 2007 period. The flat ramp transition is fixed at 15 km depth.

released by afterslip during the 1500 days following the main shock was 2.25×10^{20} N m ± 7.49×10^{19} N m, if it is considered that the main source of uncertainty is the depth of the lower tip of the flats, known to within 5 km. This value represents 56 ± 19% of the coseismic moment estimated at 3.96×10^{20} N m by *Pathier et al.* [2006]. This large value is explained mainly by the large area affected by afterslip (40 × 86 and 40 × 86 km). This ratio is significantly larger than the 13% estimated for the Chi-Chi earthquake [*Hsu et al.*, 2007] for the 15 months following the main shock and larger than the 13% estimated for the Chengkung earthquake over a 157 day period [*Hsu et al.*, 2009], if we consider postseismic displacements following ruptures along the thrust. This large value is not a result of anomalous postseismic displacements but mainly the result of the large area of the flat affected by these displacements.

[36] This major afterslip is mainly aseismic, the moment released by aftershocks during the same period being only 1.21×10^{19} N m, which represent a ratio between the cumulative moment of the aftershocks and the postseismic moment deduced from geodesy of 0.05. For comparison this ratio is also less than 0.1 in the case of the Izmit [*Reilinger et al.*, 2000] and Hector Mine [*Jacobs et al.*, 2002] earthquakes, about 0.22 for the Landers [*Shen et al.*, 1994], and 0.75 for the Chi-Chi earthquake [*Hsu et al.*, 2002].

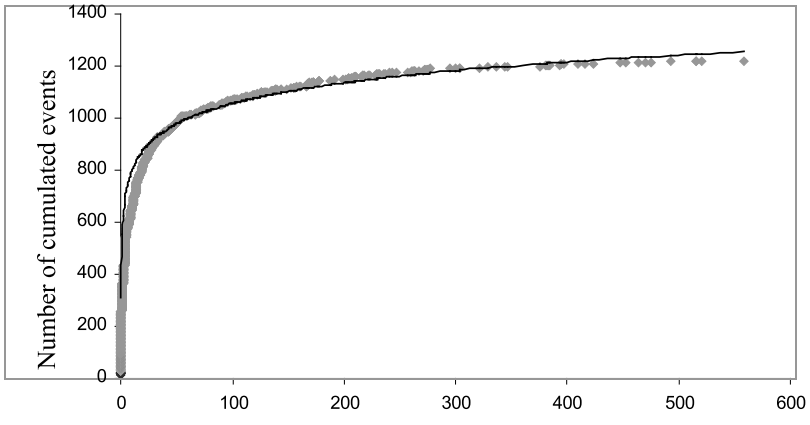

Figure 15. Cumulative number of aftershocks (gray squares) with mb > 3.5 as a function of days following the Kashmir earthquake. The function that best fits the earthquake distribution (continuous line) is obtained for tr = 8.8 years, d = 24912.233 and R0 = 0.08. R0 was obtained from the microseismicity catalogue for events with mb > 3.5 prior to the main shock.

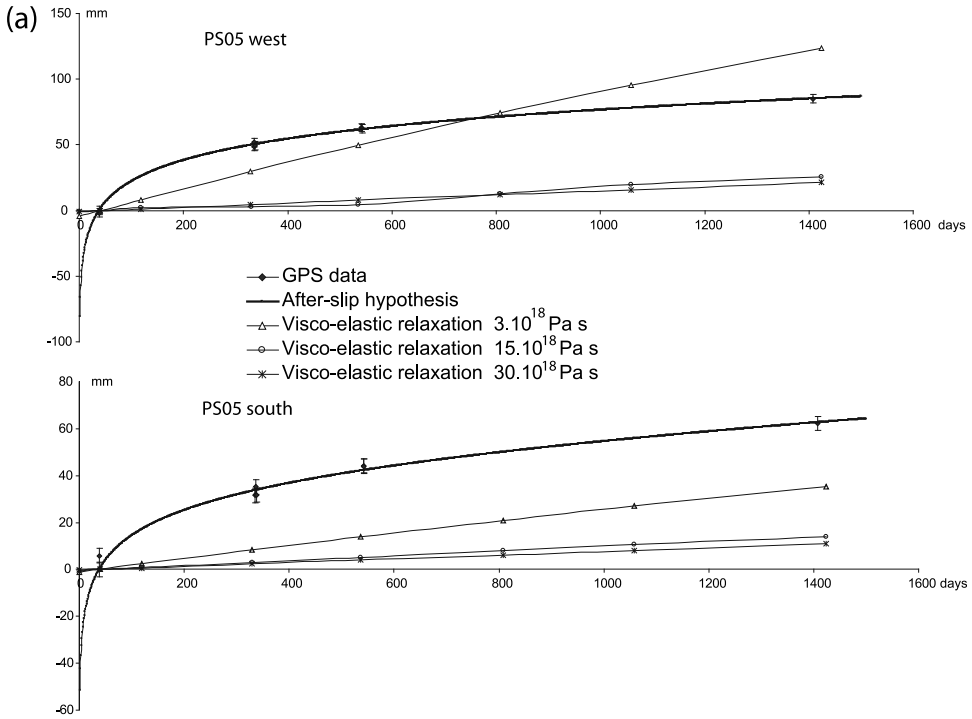

Figure 16. Observed postseismic displacements over time after the main shock and predicted displacements by equation (1) with a characteristic time tr = 8.8 years determined by analyzing aftershock distribution in time. For each component of each site the geometric factors α and β were determined by minimizing the predicted and observed displacement. The predicted times series using a viscoelastic model with viscosity of 3×10^{18} Pa s (best fit for the November 2005 to August 2006 period), 15×10^{18} Pa s (best fit for the August 2006 to March 2007 period), and 30×10^{18} Pa s (best fit for the March 2007 to August 2009 period) are plotted. The major misfits between observed and predicted time series with this viscoelastic modeling showed that viscoelastic relaxation with a Newtonian viscosity does not explain the observations or that the lower crust exhibits non-Newtonian viscosity with a nonlinear law. It must nevertheless be noted that after a year of postseismic displacements the form of the predicted time series using viscous relaxation with 15×10^{18} Pa s (best fit for the August 2006 to March 2007 period) and 30×10^{18} Pa s (best fit for the March 2007 to August 2009 period) and the observations are relatively concordant.

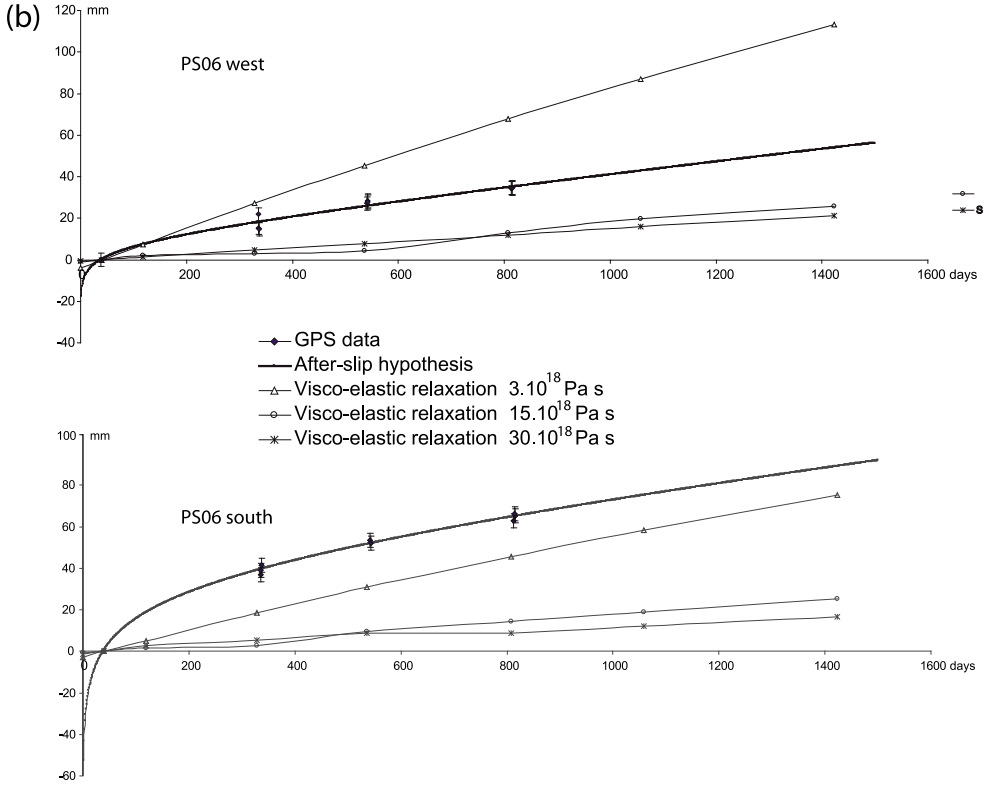

Figure 16. (continued)

[37] Following this hypothesis that aftershocks are driven by afterslip, we computed the Coulomb stress changes induced by these afterslips in thrusts with an orientation and dip similar to the main shock. We considered a regional stress with ó1 perpendicular to the strike of the Balakot-Bagh thrust, ó2 along the strike of the fault and ó3 vertical as suggested by *Parsons et al.* [2006]. Estimating the Coulomb stress enables the spatial distribution of the aftershocks to be relatively well simulated and its asymmetry to be understood. The aftershocks are mainly located northwest of the Balakot-Bagh thrust, in the Indus-Kohistan Seismic Zone [*Armbruster et al.*, 1978; *Seeber and Armbruster*, 1979; *Seeber et al.*, 1981], where the Coulomb stress increase induced by afterslip is considerable for depths of 0–8 km (Figure 17). As a conclusion, Coulomb stress change estimations underline the fact that aftershocks may be induced by afterslip along the flats north of the ramp affected by the main shock. The preexisting Indus-Kohistan Zone may also explain the observed asymmetry in the spatial distribution of the aftershocks.

7.3. Comparison Between the Viscous Relaxation Hypothesis and the Afterslip Hypothesis

[38] The residual misfits of the observed and simulated displacements for these two hypotheses (Figure 10) indicate that the dislocation hypothesis simulates the observations more effectively than the viscous relaxation hypothesis for the two first time spans (November 2005 to August 2006 and August 2006 to March 2007), whereas the residual misfits are similar for the last time span (March 2007 to August 2009). The observed and predicted time series (Figure 16) indicate that the hypothesis that afterslip is governed by a rate-strengthening friction law (the *Perfettini and Avouac* [2004] model) models the observed time series better than the viscous relaxation hypothesis, but the slopes of the predicted time series for 15×10^{18} and 30×10^{18} Pa s are close to the observed time series after 1 year of postseismic deformation. It is therefore impossible to rule out the assumption that during the first few months afterslip is the dominant mechanism, as proposed by *Hsu et al.* [2007] for the 1999 Chi-Chi earthquake in Taiwan and that, after 1 year, postseismic deformation may also be controlled by viscous relaxation, as has been proposed for postseismic deformation following the 1999 M 7.4 Izmit earthquake [*Wang et al.*, 2009].

8. Conclusions

[39] GPS measurements repeated over the 4 years following the 8 October 2005 earthquake demonstrate the occurrence of major postseismic displacements decreasing through time in the hanging wall of the Balakot-Bagh thrust.

[40] We tested two hypotheses concerning the origin of these postseismic displacements: viscous relaxation of the middle and lower crust or deep afterslip. Modeling of the viscous relaxation of the middle and lower crust does not

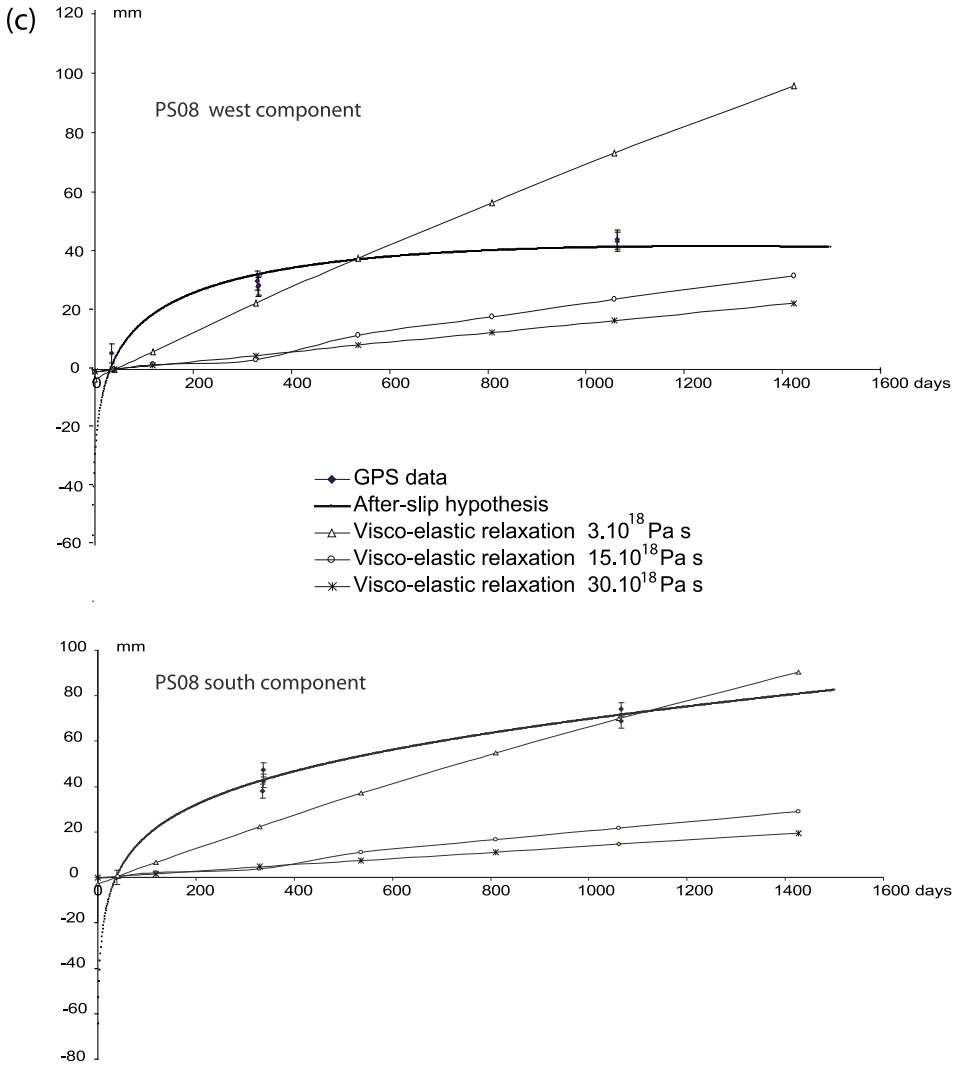

Figure 16. (continued)

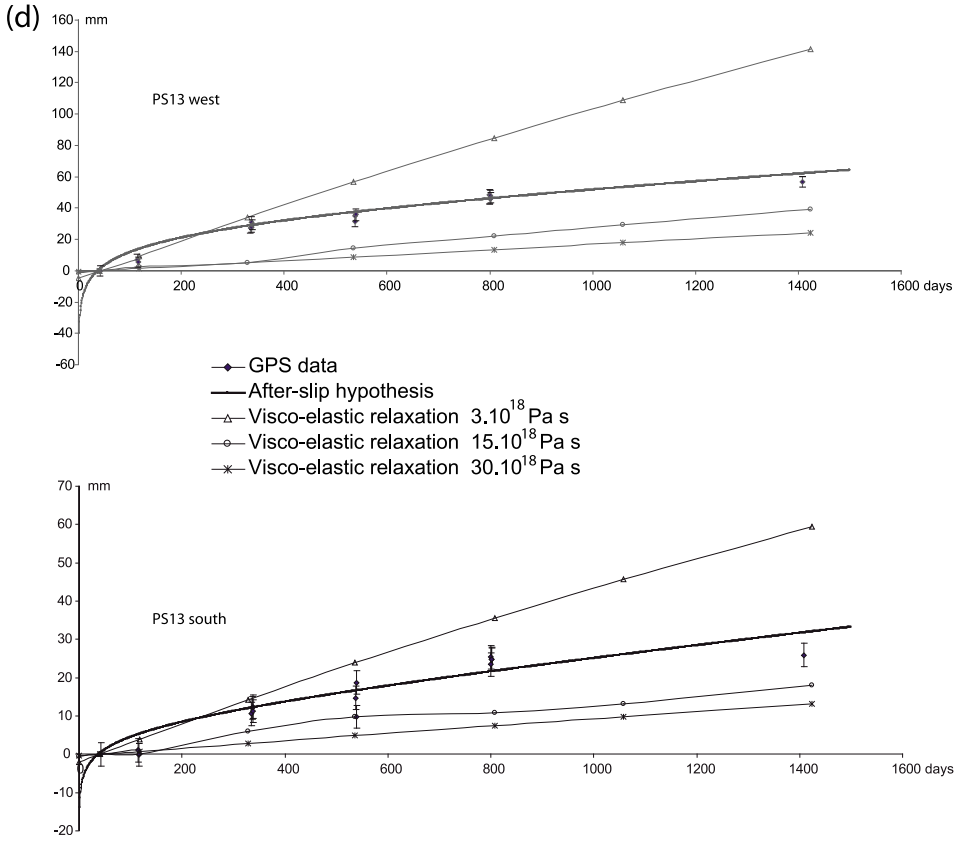

Figure 16. (continued)

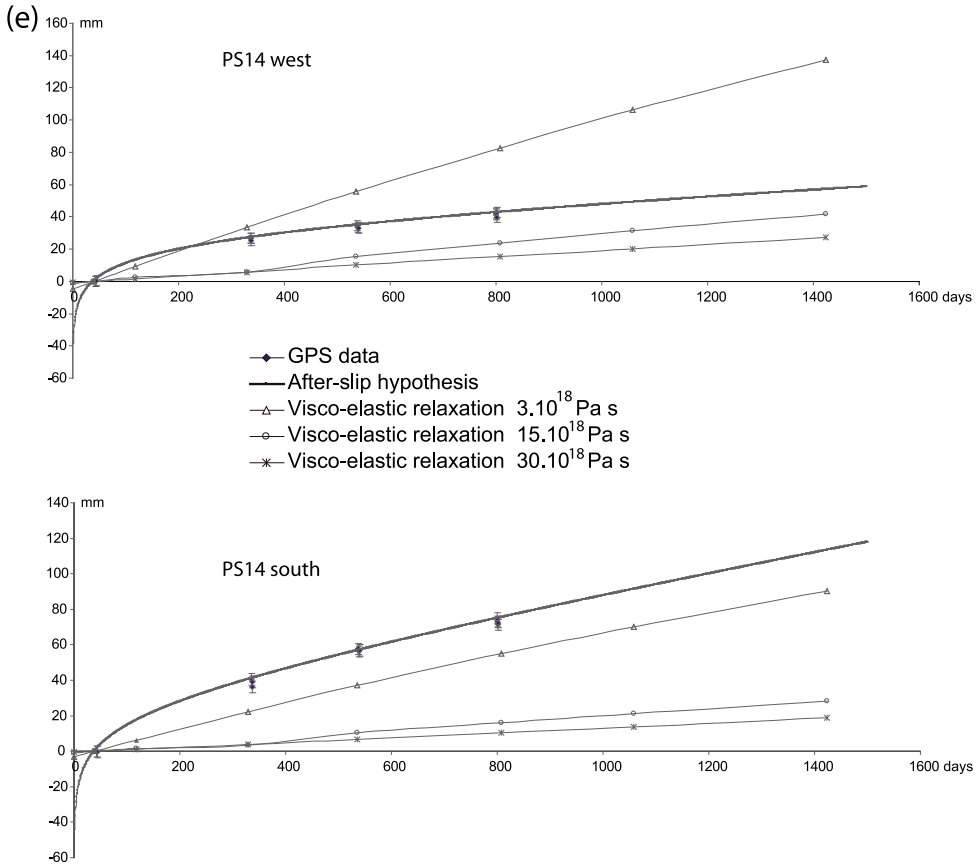

Figure 16. (continued)

yield a single Newtonian viscosity for the different time spans, so the hypothesis of Newtonian viscous relaxation of the middle and lower crust as the only origin of the postseismic displacements must therefore be rejected. Postseismic displacements may perhaps be controlled by a non-Newtonian viscosity or by afterslip along the thrust plane. By modeling these displacements it is possible to propose the occurrence of afterslip along a flat northeast of the ramp, which is separated into two parts, a northwestern one affected by major slip reaching 285 mm, and a southeastern one affected by 130 mm slip between November 2005 and August 2006. The occurrence of afterslip located mainly along a flat while no significant afterslip occurred on the ramp ruptured by coseismic displacement was observed in Taiwan after the 1999 Chi-Chi earthquake.

[41] Using the 1-D model developed by *Perfettini and Avouac* [2004], we tested the hypothesis that the aftershock distribution over time is controlled by the occurrence of such deep afterslip. This hypothesis implies that the characteristic time of the aftershock distribution and GPS time series should be the same, with the surface displacements revealing the decrease in deep afterslip.

[42] The characteristic time was determined with the aftershock distribution and, as a second step, compared with the time series. The good fit between the observed and predicted GPS time series validates the assumption that the

Table 6. Ratio Between Estimated Postseismic Displacements for the First 1500 Days Following the Earthquake and the Observed Postseismic Displacements for the November 2005 to August 2006 period[a]

	East D0-1500	North D0-1500	East: November 2005 to August 2006	North: November 2005 to August 2006	East Ratio	North Ratio
PS04	171.0	25.0	56.9	10.5	3.01	2.38
PS05	167.7	115.7	50	29.8	3.35	3.88
PS06	73.8	144.4	16.8	37.5	4.39	3.85
PS08	98.8	146.8	23.5	41.5	4.20	3.54
PS13	104.0	47.0	28.5	11.4	3.65	4.13
PS14	97.2	162.2	25.4	37.9	3.83	4.28
Mean value					3.74	3.68
Adopted value					3.71	

[a]Cumulative slip along dislocations for the 1500 days following the earthquake is thus 3.71 larger than the slip estimated for the November 2005 to August 2006 period.

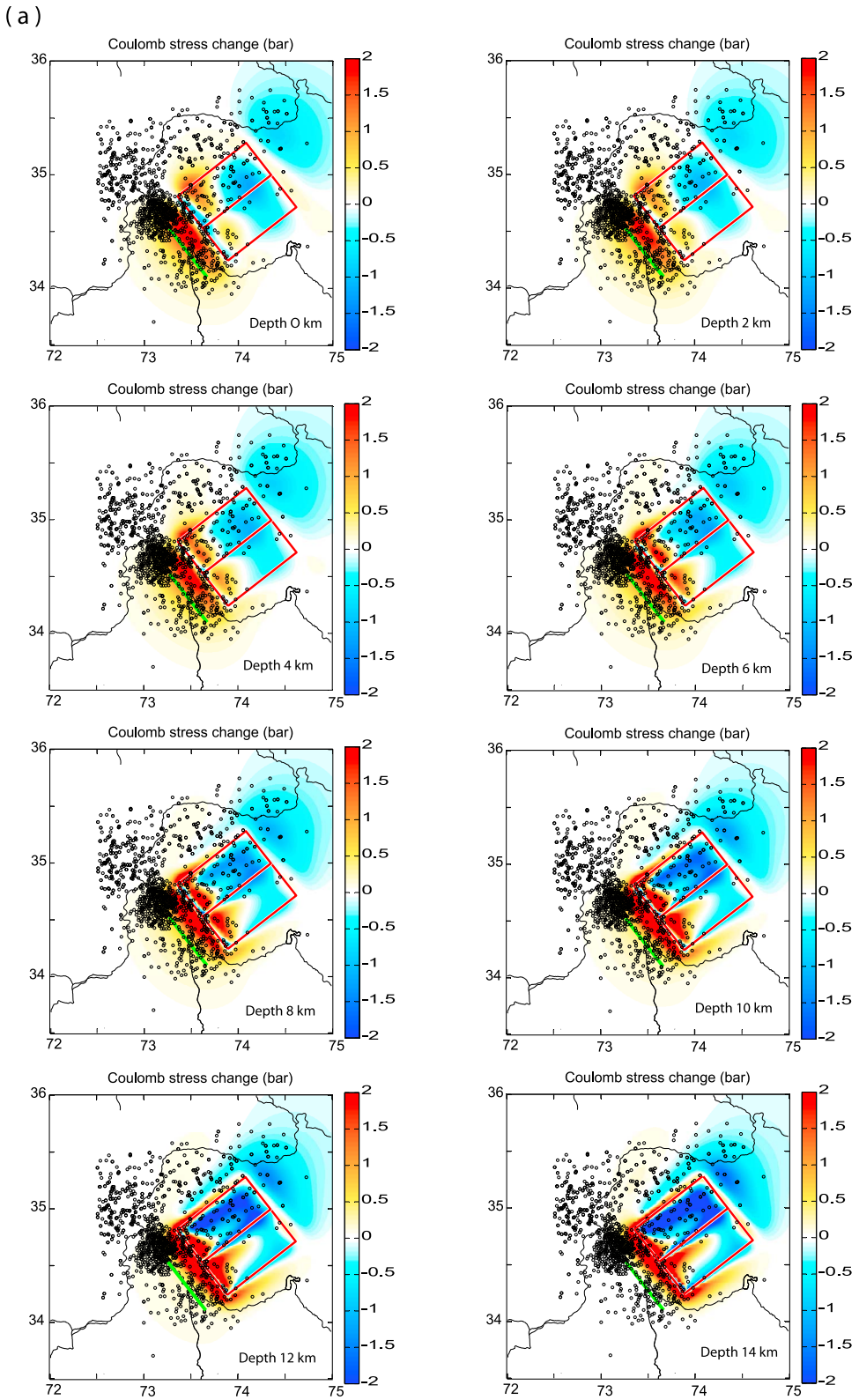

Figure 17. Coulomb stress change induced by total afterslip along the flats. (a) Coulomb stress change was estimated for 142°N thrusts dipping 30° northeastward, for a 0.4 friction ratio using Coulomb 3.1 software [*Toda et al.*, 2005; *Lin and Stein*, 2004] for different depths, and (b) zoom of Coulomb stress change for the surface.

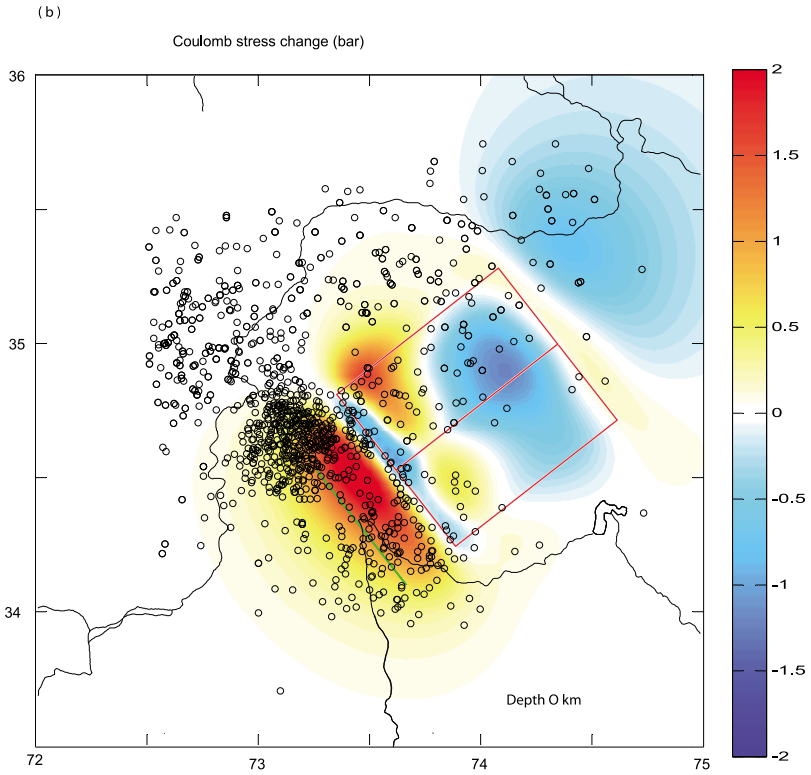

Figure 17. (continued)

occurrence of aftershocks is directly governed by deep afterslip and allows the early postseismic displacement between the main shock and the first GPS measurements to be estimated. Coulomb stress changes induced by these afterslips in the case of thrusts with the same orientations, dip and rake as the main shock may explain the spatial distribution of the aftershocks, which reinforces the hypothesis of a direct link between afterslip and aftershocks. The seismic moment released by the afterslip, which is mainly aseismic, reaches 56 ± 19% of the seismic moment released by the main shock. This high value mainly reflects the large area of flat affected by afterslip.

[43] Our estimate of the characteristic relaxation time (8.8 years) appears to be close to the 8.5 years estimated by *Perfettini and Avouac* [2004] for the Chi-Chi earthquake in a similar tectonic context and to the previous estimates of 7–11 years given by *Parsons* [2002] for global triggered earthquakes or 10.2 years for shallow earthquakes [*Dieterich*, 1994]. It may therefore be proposed that brittle creep of a flat could be a common mechanism controlling the change in seismicity over time, particularly in the case of a fault located in the upper crust, ruptured by a major earthquake and connected to a deep flat.

[44] This comparison between the two mechanisms of viscous relaxation and afterslip shows that afterslip better explains the observations. Nevertheless, we can rule out afterslip as the dominant mechanism during the first year as also proposed by *Reddy and Prajapati* [2008] with CGPS data for the first 8 months of postseismic deformation, whereas, subsequently, viscous relaxation may perhaps also contribute to postseismic deformation.

[45] **Acknowledgments.** The authors wish to thank the PAKSIS program of the ANR Catel for funding the present research. They also wish to thank the French Embassy in Pakistan for its constant support, especially Sonia Darcaq, who was in charge of scientific collaboration at the beginning of this program. Thanks are also due to the Geological Survey of Pakistan and the Ministry of Mines and Petroleum Resources for their useful help with customs formalities and field acquisitions. The authors also wish to thank the Associate Editor and two anonymous reviewers for their helpful comments and suggestions.

References

Altamimi, Z., X. Collilieux, J. Legrand, B. Garayt, and C. Boucher (2007), ITRF2005: A new release of the International Terrestrial Reference Frame based on time series of station positions and Earth Orientation Parameters, *J. Geophys. Res.*, *112*, B09401, doi:10.1029/2007JB004949.

Armbruster, J., L. Seeber, and K. H. Jacob (1978), The northwestern termination of the Himalayan mountain front: Active tectonics from microearthquakes, *J. Geophys. Res.*, *83*, 269–282, doi:10.1029/JB083iB01p00269.

Avouac, J.-P., F. Ayoub, S. Leprince, O. Konca, and D. V. Helmberger (2006), The 2005, *Mw* 7.6 Kashmir earthquake: Sub-pixel correlation of ASTER images and seismic waveforms analysis, *Earth Planet. Sci. Lett.*, *249*, 514–528, doi:10.1016/j.epsl.2006.06.025.

Banerjee, P., F. Pollitz, and R. Bürgmann (2007), Coseismic slip distributions of the 26 December 2004 Sumatra-Andaman and 28 March 2005 Nias earthquakes from GPS static offsets, *Bull. Seismol. Soc. Am.*, *97*, S86–S102.

Bendick, R., R. Bilham, M. Asif Khan, and S. Faisal Khan (2007), Slip on an active wedge thrust from geodetic observations of the 8 October 2005 Kashmir earthquake, *Geology*, *35*, 267–270, doi:10.1130/G23158A.1.

Bettinelli, P., J. P. Avouac, M. Flouzat, P. Willis, F. Jouanne, L. Bollinger, and G. R. Chitrakar (2006), Plate motion of India and interseismic strain

in the Nepal Himalaya from GPS and DORIS measurements, *J. Geod.*, *80*, 567–589, doi:10.1007/s00190-006-0030-3.

Beutler, G., M. Rothacher, S. Schaer, T. A. Springer, J. Kouba, and R. E. Neilan (1999), The International GPS Service (IGS): An interdisciplinary service in support of Earth sciences, *Adv. Space Res.*, *23*, 631–653, doi:10.1016/S0273-1177(99)00160-X.

Blanpied, M. L., D. A. Lockner, and J. D. Byerlee (1991), Fault stability inferred from granite sliding experiments at hydrothermal conditions, *Geophys. Res. Lett.*, *18*, 609–612, doi:10.1029/91GL00469.

Blanpied, M. L., D. A. Lockner, and J. D. Byerlee (1995), Frictional slip of granite at hydrothermal conditions, *J. Geophys. Res.*, *100*, 13,045–13,064, doi:10.1029/95JB00862.

Boucher, C., Z. Altamimi, P. Sillard, and M. Feissel-Vernier (2004), The International Terrestrial Reference Frame (ITRF2000), *IERS Tech. Note 31*, Verl. des Bundesants. fur Kartogr. und Geod., Frankfurt, Germany.

Chandrasekhar, D. V., R. Bürgmann, C. D. Reddy, P. S. Sunil, and D. A. Schmidt (2009), Weak mantle in NW India probed by geodetic measurements following the 2001 Bhuj earthquake, *Earth Planet. Sci. Lett.*, *280*, 229–235, doi:10.1016/j.epsl.2009.01.039.

Cheng, L.-W., L. Jian-Cheng, H. Jyr-Ching, and C. Horng-Yue (2009), Coseismic and post-seismic slip distribution of the 2003 *Mw* = 6.5 Chengkung earthquake in eastern Taiwan: Elastic modeling from inversion of GPS data, *Tectonophysics*, *466*, 335–343, doi:10.1016/j.tecto.2007.11.021.

Chester, F. M. (1995), A rheologic model for wet crust applied to strike-slip faults, *J. Geophys. Res.*, *100*, 13,033–13,044, doi:10.1029/95JB00313.

Dieterich, J. (1994), A constitutive law for rate of earthquake production and its application to earthquake clustering, *J. Geophys. Res.*, *99*, 2601–2618, doi:10.1029/93JB02581.

DiPietro, J., K. Pogue, A. Hussain, and I. Ahmad (1999), Geological map of the Indus syntaxis and surrounding area, northwest Himalaya, Pakistan, *Spec. Pap. Geol. Soc. Am.*, *328*, 159–178.

Frye, K. M., and C. Marone (2002), Effect of humidity on granular friction at room temperature, *J. Geophys. Res.*, *107*(B11), 2309, doi:10.1029/2001JB000654.

Fujiwara, S., et al. (2006), Satellite data gives snapshot of the 2005 Pakistan earthquake, *Eos Trans. AGU*, *87*(7), 73–77, doi:10.1029/2006EO070001.

Grelaud, S., W. Sassi, D. Frizon de Lamotte, T. Jaswal, and F. Roure (2002), Kinematics of eastern Salt Range and South Potwar Basin (Pakistan): A new scenario, *Mar. Pet. Geol.*, *19*, 1127–1139, doi:10.1016/S0264-8172(02)00121-6.

Hsu, Y.-J., N. Bechor, P. Segall, S.-B. Yu, L.-C. Kuo, and K.-F. Ma (2002), Rapid afterslip following the 1999 Chi-Chi, Taiwan, earthquake, *Geophys. Res. Lett.*, *29*(16), 1754, doi:10.1029/2002GL014967.

Hsu, Y.-J., P. Segall, S. B. Yu, L.-C. Kuo, and C. A. Williams (2007), Temporal and spatial variations of post-seismic deformation following the 1999 Chi-Chi, Taiwan, earthquake, *Geophys. J. Int.*, *169*, 367–379, doi:10.1111/j.1365-246X.2006.03310.x.

Hsu, Y.-J., Y. Shui-Beih, and C. Horng-Yue (2009), Coseismic and post-seismic deformation associated with the 2003 Chengkung, Taiwan, earthquake, *Geophys. J. Int.*, *176*, 420–430, doi:10.1111/j.1365-246X.2008.04009.x.

Hutton, W., C. DeMets, O. Sánchez, G. Suárez, and J. Stock (2001), Slip dynamics during and after the 9 October 1995 *Mw* = 8.0 Colima-Jalisco, Mexico, *Geophys. J. Int.*, *146*, 637–658, doi:10.1046/j.1365-246X.2001.00472.x.

Jacobs, A., D. Sandwell, Y. Fialko, and L. Sichoix (2002), The 1999 (*Mw* 7.1) Hector Mine, California, earthquake: Near-field post-seismic deformation from ERS interferometry, *Bull. Seismol. Soc. Am.*, *92*, 1433–1442, doi:10.1785/0120000908.

Jade, S., B. C. Bhatt, Z. Yang, R. Bendick, V. K. Gaur, P. Molnar, M. B. Anand, and D. Kumar (2004), GPS measurements from the Ladakh Himalaya, India: Preliminary tests of plate-like or continuous deformation in Tibet, *Geol. Soc. Am. Bull.*, *116*, 1385–1391, doi:10.1130/B25357.1.

Jayangondaperumal, R., and V. C. Thakur (2008), Coseismic secondary surface fractures on southeastward extension of the rupture zone of the 2005 Kashmir earthquake, *Tectonophysics*, *446*, 61–76, doi:10.1016/j.tecto.2007.10.006.

Kaneda, H., et al. (2008), Surface rupture of the 2005 Kashmir, Pakistan, earthquake, and its active tectonic implications, *Bull. Seismol. Soc. Am.*, *98*, 521–557, doi:10.1785/0120070073.

Kumar, S., S. G. Wesnousky, T. K. Rockwell, R. W. Briggs, V. C. Thakur, and R. Jayangondaperumal (2006), Paleoseismic evidence of great surface rupture earthquakes along the Indian Himalaya, *J. Geophys. Res.*, *111*, B03304, doi:10.1029/2004JB003309.

Lavé, J., D. Yule, S. Sapkota, K. Basenta, C. Madden, M. Attal, and R. Pandey (2005), Evidence for a great medieval earthquake (~A.D. 1100) in central Himalaya, Nepal, *Science*, *307*, 1302–1305, doi:10.1126/science.1104804.

Lin, J., and R. S. Stein (2004), Stress triggering in thrust and subduction earthquakes and stress interaction between the southern San Andreas and nearby thrust and strike-slip faults, *J. Geophys. Res.*, *109*, B02303, doi:10.1029/2003JB002607.

Mahsas, A., K. Lammali, K. Yelles, E. Calais, A. M. Freed, and P. Briole (2008), Shallow afterslip following the 2003 May 21, *M*w = 6.9 Boumerdes earthquake, Algeria, *Geophys. J. Int.*, *172*, 155–166, doi:10.1111/j.1365-246X.2007.03594.x.

Marone, C. (1998), Laboratory-derived friction laws and their application to seismic faulting, *Annu. Rev. Earth Planet. Sci.*, *26*, 643–696, doi:10.1146/annurev.earth.26.1.643.

McDougall, J. W., and S. H. Khan (1990), Strike-slip faulting in a foreland fold-thrust belt: The Kalabagh Fault and Western Salt Range, Pakistan, *Tectonics*, *9*, 1061–1075, doi:10.1029/TC009i005p01061.

McDougall, J. W., A. Hussain, and R. S. Yeats (1993), The main boundary thrust and propagation of deformation into the foreland fold and thrust belt in northern Pakistan near the Indus River, *Spec. Publ. Geol. Soc. London*, *74*, 581–588.

Melbourne, W. G. (1985) The case for ranging in GPS based geodetic system, paper presented at 1st International Symposium on Precise Positioning with the Global Positioning System, Int. Assoc. of Geod., Rockville, Md.

Mugnier, J.-L., P. Huyghe, P. Leturmy, and F. Jouanne (2004), Episodicity and rates of thrust-sheet motion in the Himalayas (western Nepal), in *Thrust Tectonics and Hydrocarbon Systems*, *AAPG Mem.*, vol. 82, edited by K. R. McClay, pp. 91–114, Am. Assoc. of Pet. Geol., Tulsa, Okla.

Mugnier, J. L., J. Carcaillet, F. Jouanne, S. Lataud, A. Pêcher, A. Kausar, A. Majid, and M. Mughai (2008), A comparison between the kinematic rates of the Salt Range and the Siwalik thrust belt: Seismic hazard implications, paper presented at Workshop on the October 8, 2005, Kashmir Earthquake and After, Indian Geol. Congr., Jammu, India.

Okada, Y. (1985), Surface deformation due to shear and tensile faults in a half-space, *Bull. Seismol. Soc. Am.*, *75*, 1135–1154.

Parsons, T. (2002), Global Omori law decay of triggered earthquakes: Large aftershocks outside the classical aftershock zone, *J. Geophys. Res.*, *107*(B9), 2199, doi:10.1029/2001JB000646.

Parsons, T., R. S. Yeats, Y. Yagi, and A. Hussain (2006), Static stress change from the 8 October, 2005 M = 7.6 Kashmir earthquake, *Geophys. Res. Lett.*, *33*, L06304, doi:10.1029/2005GL025429.

Pathier, E., E. J. Fielding, T. J. Wright, R. Walker, B. E. Parsons, and S. Hensley (2006), Displacement field and slip distribution of the 2005 Kashmir earthquake from SAR imagery, *Geophys. Res. Lett.*, *33*, L20310, doi:10.1029/2006GL027193.

Pennington, W. D. (1989), A summary of field and seismic observations of the Pattan earthquake—28 December 1974, in *Geodynamics of Pakistan*, edited by A. Farah and K. A. DeJong, pp. 143–147, Geol. Surv. of Pakistan, Quetta.

Perfettini, H., and J.-P. Avouac (2004), Postseismic relaxation driven by brittle creep: A possible mechanism to reconcile geodetic measurements and the decay rate of aftershocks, application to the Chi-Chi earthquake, Taiwan, *J. Geophys. Res.*, *109*, B02304, doi:10.1029/2003JB002488.

Pollitz, F. F. (1997), Gravitational viscoelastic postseismic relaxation on a layered spherical Earth, *J. Geophys. Res.*, *102*, 17,921–17,941, doi:10.1029/97JB01277.

Pollitz, F. F. (2003), Transient rheology of the uppermost mantle beneath the Mojave Desert, California, *Earth Planet. Sci. Lett.*, *215*, 89–104, doi:10.1016/S0012-821X(03)00432-1.

Pollitz, F. F., C. Wicks, and W. Thatcher (2001), Mantle flow beneath a continental strike-slip fault: Postseismic deformation after the 1999 Hector Mine earthquake, *Science*, *293*, 1814–1818, doi:10.1126/science.1061361.

Rai, S. S., K. Priestley, V. K. Gaur, S. Mitra, M. P. Singh, and M. Searle (2006), Configuration of the Indian Moho beneath the NW Himalaya and Ladakh, *Geophys. Res. Lett.*, *33*, L15308, doi:10.1029/2006GL026076.

Reddy, C. D., and S. K. Prajapati (2008), GPS measurements of postseismic deformation due to October 8, 2005 Kashmir earthquake, *J. Seismol.*, *13*, 415–420, doi:10.1007/s10950-008-9111-5.

Reilinger, R. E., et al. (2000), Coseismic and postseismic fault slip for the 17 August 1999, *M* = 7.5, Izmit, Turkey, earthquake, *Science*, *289*, 1519–1524, doi:10.1126/science.289.5484.1519.

Seeber, L., and J. Armbruster (1979), Seismicity of the Hazara Arc in northern Pakistan: decollement vs. basement faulting, in *Geodynamics of Pakistan*, edited by A. Farah and K. A. DeJong, pp. 131–142, Geol. Surv. of Pakistan, Quetta.

Seeber, L., J. Armbruster, and R. Quittmeyer (1981), Seismicity and continental collision in the Himalayan arc, in *Zagros, Hindukush, Himalaya:*

Geodynamic Evolution, *Geodyn. Ser.*, vol. 3, edited by H. K. Gupta and F. M. Delany, pp. 215–242, AGU, Washington, D. C.

Shen, Z.-K., D. D. Jackson, Y. Feng, M. Cline, M. Kim, P. Feng, and Y. Bock (1994), Postseismic deformation following the Landers earthquake, California, 28 June 1992, *Bull. Seismol. Soc. Am.*, *84*, 780–791.

Srinivasan, S., and B. M. Khar (1996), Status of hydrocarbon exploration in northwest Himalaya and foredeep: Contribution to stratigraphy and structure, *Geol. Surv. Ind. Spec. Publ.*, *21*, 295–405.

Toda, S., R. S. Stein, K. Richards-Dinger, and S. B. Bozkurt (2005), Forecasting the evolution of seismicity in Southern California: Animations built on earthquake stress transfer, *J. Geophys. Res.*, *110*, B05S16, doi:10.1029/2004JB003415.

Wang, L., R. Wang, F. Roth, B. Enescu, S. Hainzl, and S. Ergintav (2009), Afterslip and viscoelastic relaxation following the 1999*M* 7.4 İzmit earthquake from GPS measurements, *Geophys. J. Int.*, *178*, 1220–1237, doi:10.1111/j.1365-246X.2009.04228.x.

Williams, S. D. P., Y. Bock, P. Fang, P. Jamason, R. M. Nikolaidis, L. Prawirodirdjo, M. Miller, and D. J. Johnson (2004), Error analysis of continuous GPS position time series, *J. Geophys. Res.*, *109*, B03412, doi:10.1029/2003JB002741.

Wübbena, G. (1985), Software developments for geodetic positioning with GPS using TI4100 code and carrier measurements, paper presented at 1st International Symposium on Precise Positioning with the Global Positioning System, Int. Assoc. of Geod., Rockville, Md.

Yu, S.-B., Y.-J. Hsu, L.-C. Kuo, H.-Y. Chen, and C.-C. Liu (2003), GPS measurement of postseismic deformation following the 1999 Chi-Chi, Taiwan, earthquake, *J. Geophys. Res.*, *108*(B11), 2520, doi:10.1029/2003JB002396.

Zhang, J., Y. Bock, H. Johnson, P. Fang, S. Williams, J. Genrich, S. Wdowinski, and J. Behr (1997), Southern California Permanent GPS Geodetic Array: Error analysis of daily position estimates and site velocities, *J. Geophys. Res.*, *102*, 18,035–18,055, doi:10.1029/97JB01380.

A. Awan, A. Kausar, N. A. Khan, M. Latif, and A. Madji, Geological Survey of Pakistan, Plot 84, H-8/1 Islamabad, Pakistan.

F. Jouanne and J. L. Mugnier, ISterre, UMR 5275, Université de Savoie, CNRS, Campus Scientifique, F-73376 Le Bourget du Lac, France. (fjoua@univ-savoie.fr)

I. Khan, Geological Survey of Pakistan, Sariab Road, Quetta, Pakistan.

A. Pêcher, ISterre, UMR 5275, Université Joseph Fourier, BP 53, F-38041 Grenoble, France.